Recent Advances in High Resolution Rotation Sensing

U. Schreiber[1,2], A. Gebauer[1], R. Hurst[2], J.-P. Wells[2]

[1]Forschungseinrichtung Satellitengeodäsie,
Technische Universität München, Germany

[2]Department of Physics and Astronomy
University of Canterbury, Christchurch, NZ

Over the recent years we have improved the ring laser technology by as much as a factor of 3 in sensitivity, which made the domain of $\Delta\Omega/\Omega \approx 10^{-9}$ of Earth rotation accessible to a local rotation sensor. Currently it appears that the micro-seismic background activity of the Earth causes the major part from the observed deviation of the sensor performance with respect to the computed shot noise limit. Recent efforts concentrated on the improvement of the sensor stability against drift effects caused by the aging of the laser gas, scale factor instabilities induced by atmospheric pressure variations and the corresponding temperature changes from adiabatic expansion and compression of the local air around the instrument. The extension of the regime of stability gives access to geophysical signals at frequencies substantially lower than previously observable with ring lasers. This talk outlines this recent progress in Sagnac interferometry and presents the new data.

"Requirements for Space Geodesy" or what was the motivation to build large ring lasers

- Establishment of exact positions and the structure of extra-galactic radio sources (Quasars)
- Determination of precise global, regional and local 3D coordinates
- Determination of the instantaneous Earth rotation axis and the rate of rotation as a function of time. (This allows the transformation between terrestrial and celestial reference frame)
- Determination of the Gravity Field of the Earth and its variation with time.

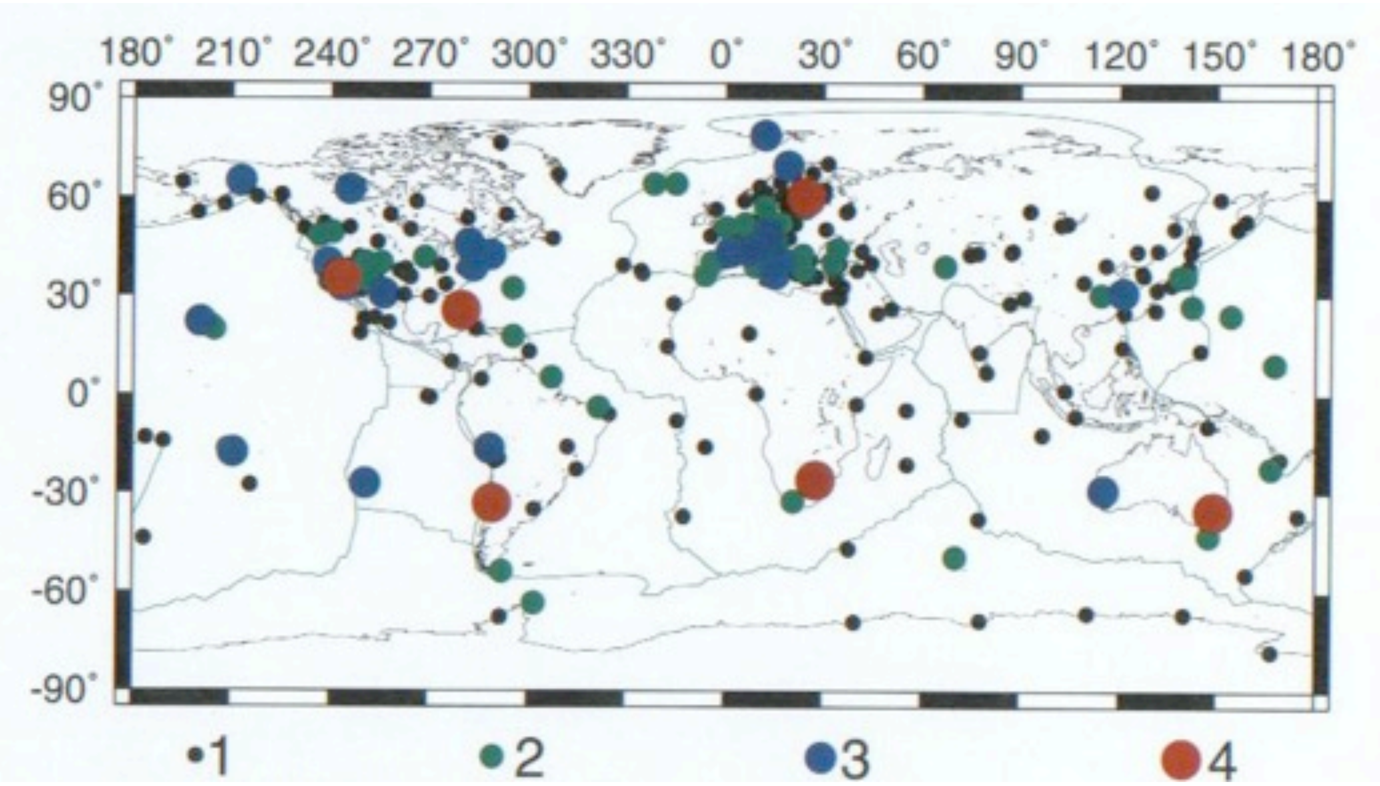

ITRF: Earth fixed Reference Frame

ICRF: Space fixed Reference Frame

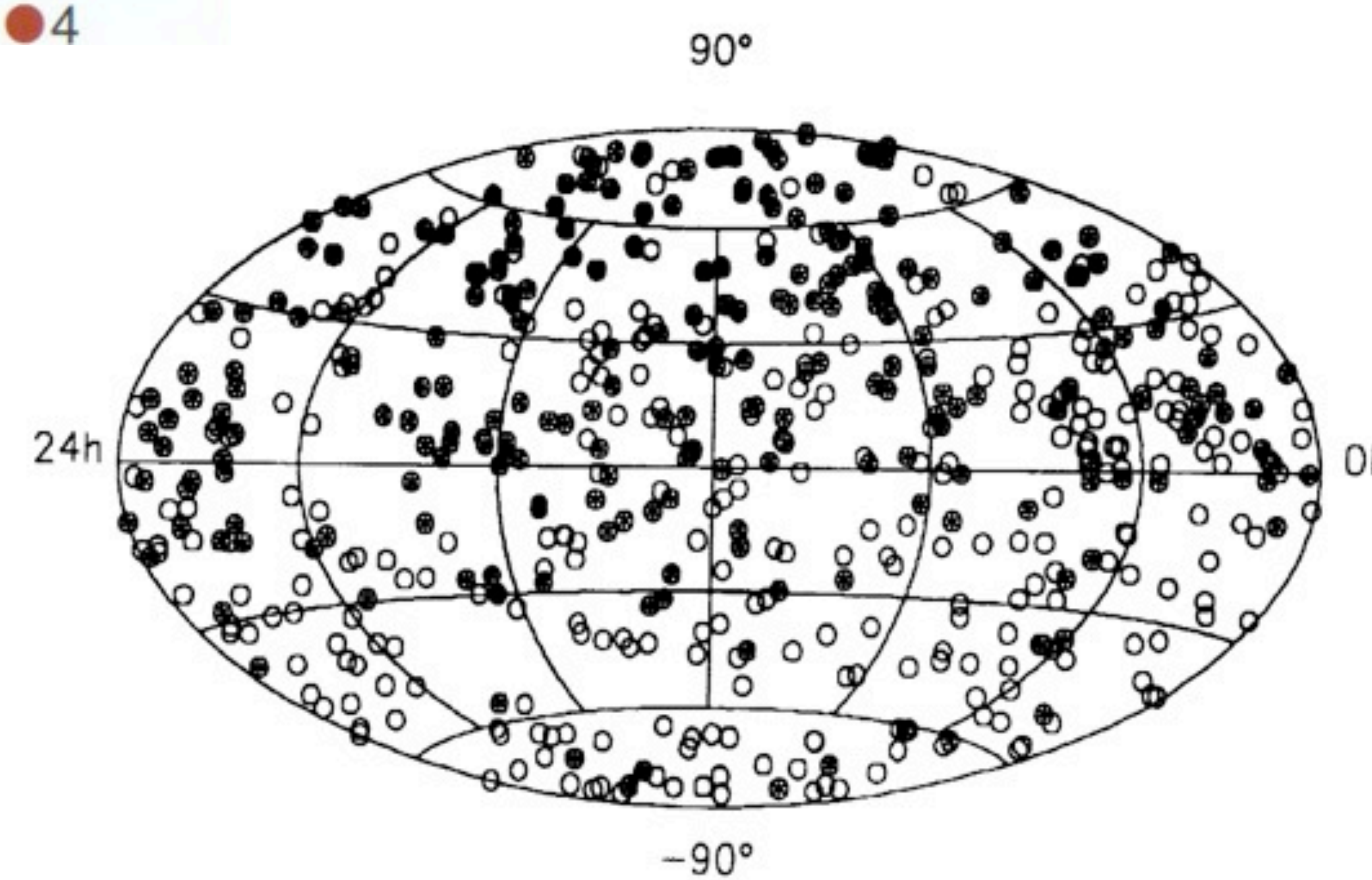

… and Earth rotation as the link between them

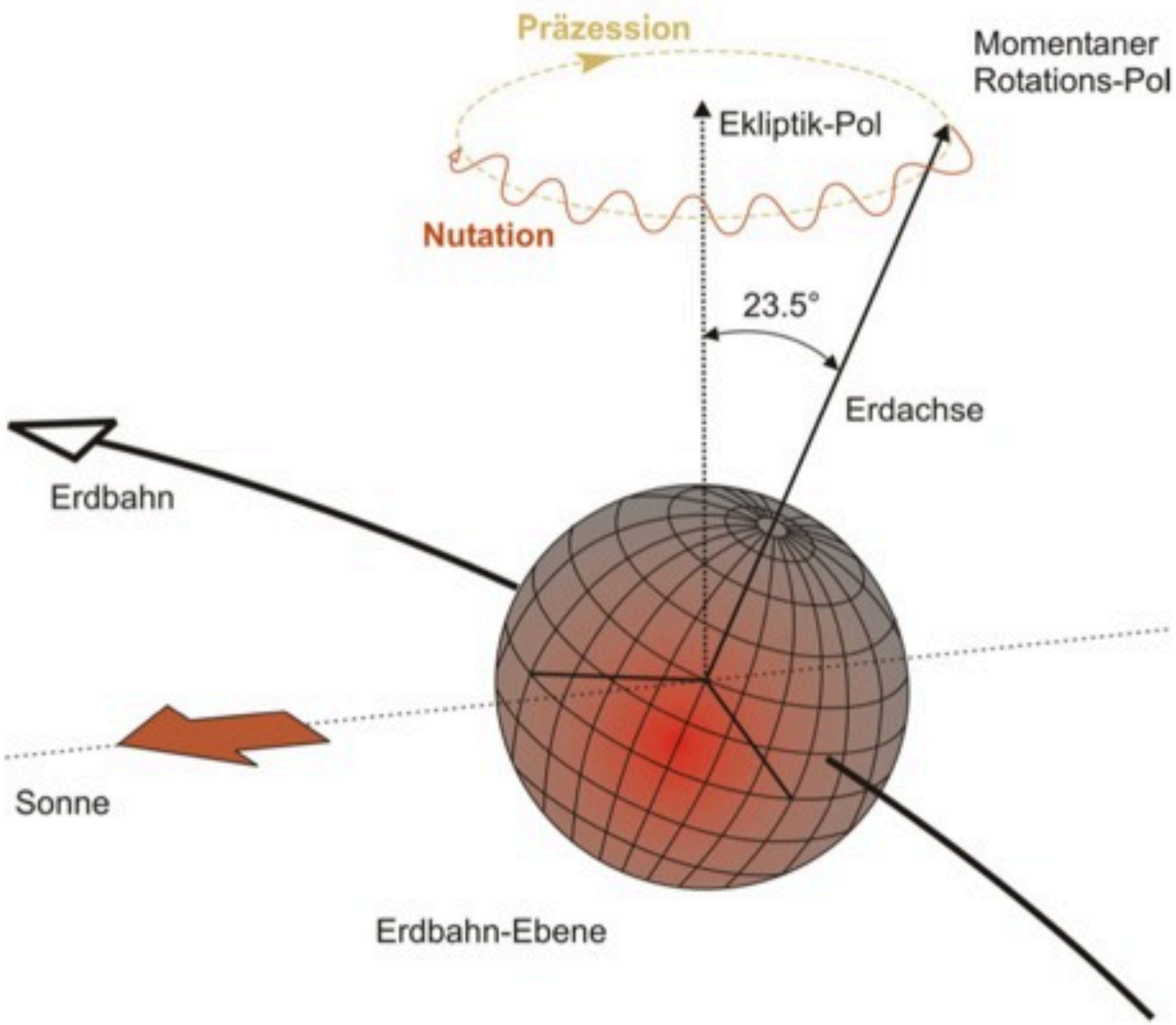

a) the rotation rate of the Earth is not constant. Deceleration by dissipation and variation by momentum exchange. Free oscillations excited by ocean, atmosphere

b) gravitational attraction of sun and moon on a near spherical object give rise to precession and nutation

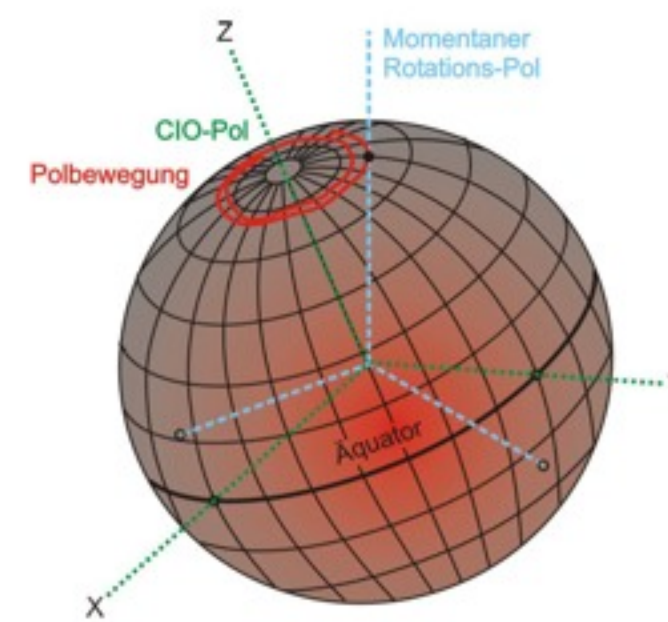

c) mass redistribution on Earth and the fact that the figure axis and the axis of Inertia are not coinciding, give rise to polar motion

Linking Celestial and Terrestrial Reference Frames

Star Compass

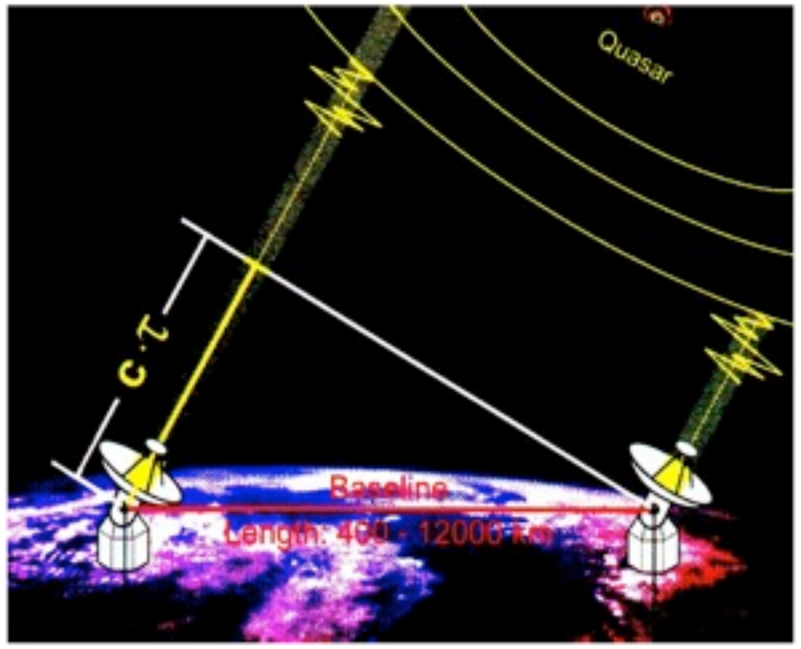

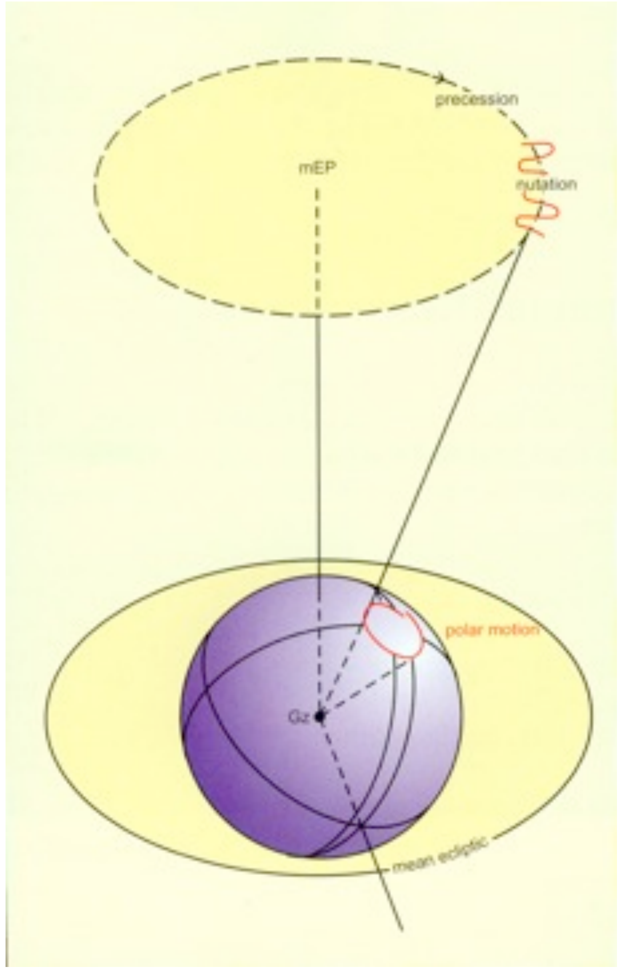

Earth Rotation Orientation

Inertial Compass

Requirements

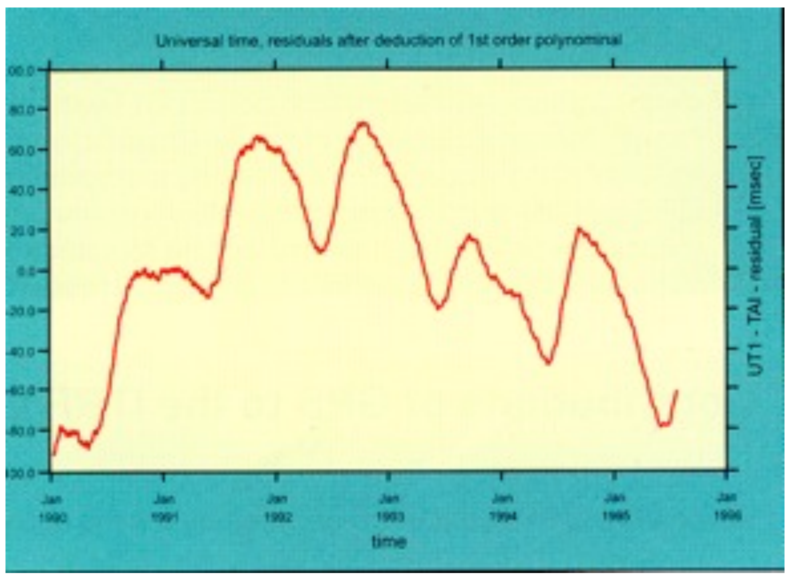

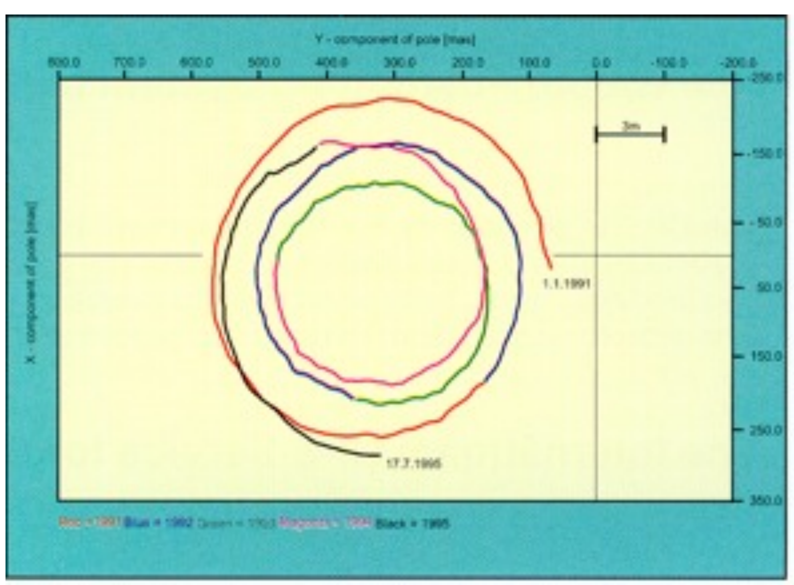

- LoD ≈ 0.05 ms
- Drift < 10^{-9} Ω_E over Months (Chandler Wobble)
- Orientation ≈ 1 nrad (1 cm) (Polar Motion)

Sagnac Interferometer (1913)

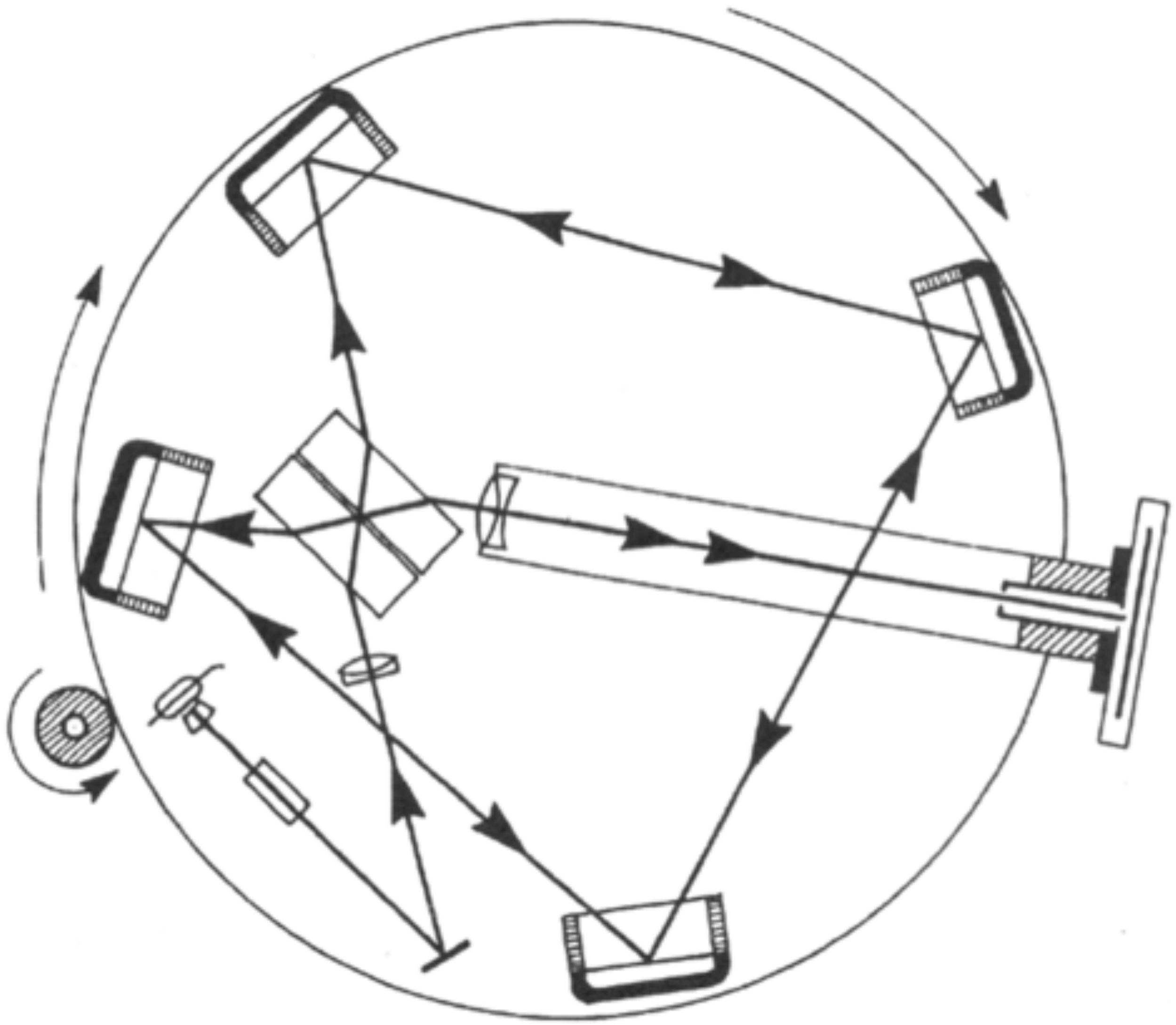

GP-B: 10^{-8} °/h ≈ 5 x 10^{-14} rad/s

PASSIVE

FOG: (large scale factor... but sensitivity, stability insufficient for Geoscience)

externally injected stabilized laser beams: (concept shown, backscatter issues similar to RLG...)

ACTIVE

Ring Laser: operational

1.2 x 10^{-11} rad/s/sqrt(Hz) (PRL 107, 173904 (2011))

---

atom interferom.: (short-term)

6 x 10^{-10} rad/s (Class. Quant. Grav. **17** (2000) 2385–2398)

Josephson effect: delicate + small,

8 x 10^{-9} rad/s/sqrt(Hz) (Rep. Prog. Phys. **75** (2012) 016401)

Ring Laser Block Diagram

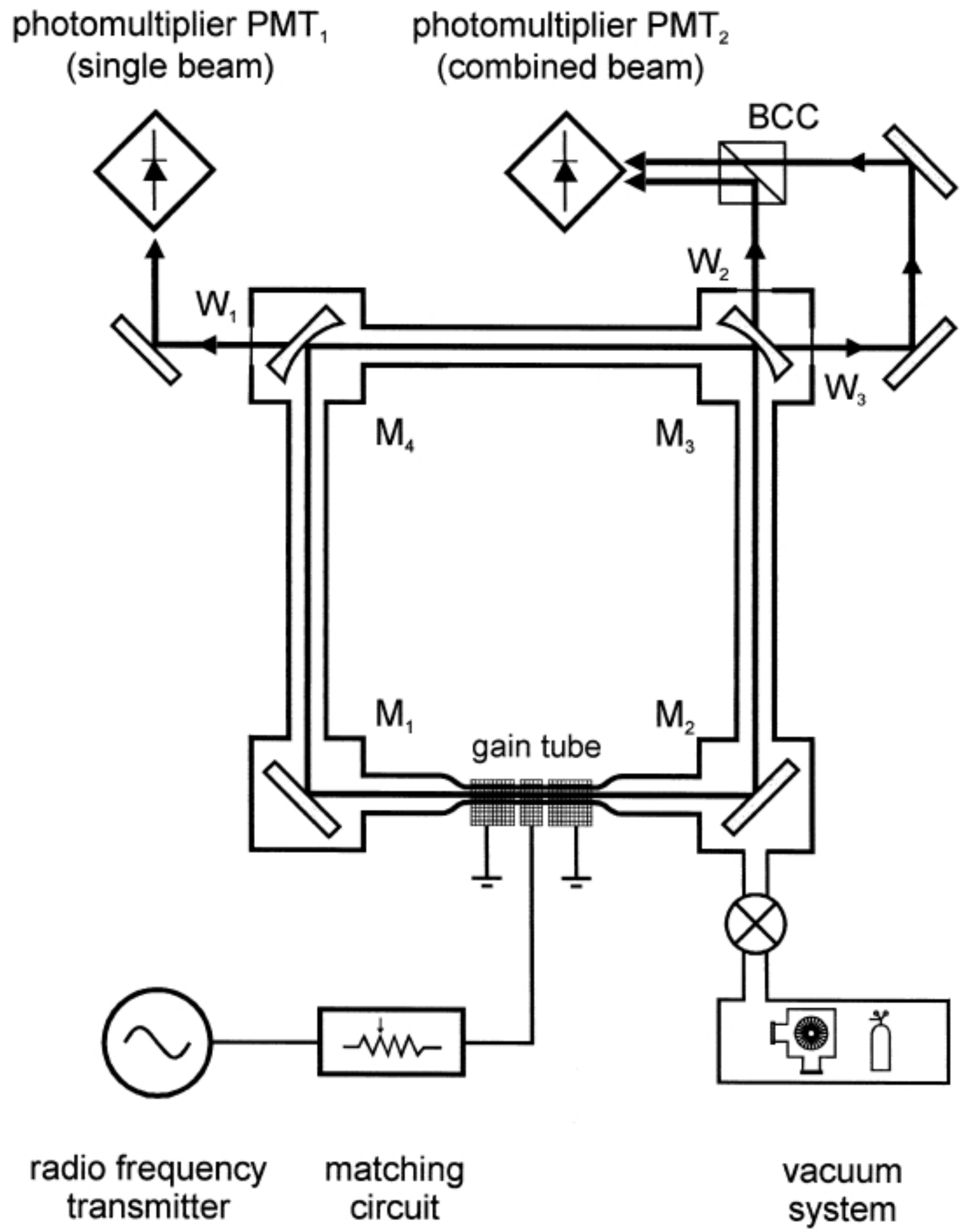

Ring Laser Essentials

A ring laser gyroscope is defined by a closed light path

It is the entire apparatus that rotates (strap down)

The sensitivity is given by the scale factor

$$S = \frac{4A}{\lambda P}$$

Entirely insensitve to translations

linear transfer function

Rotation signal encoded in frequency modulation

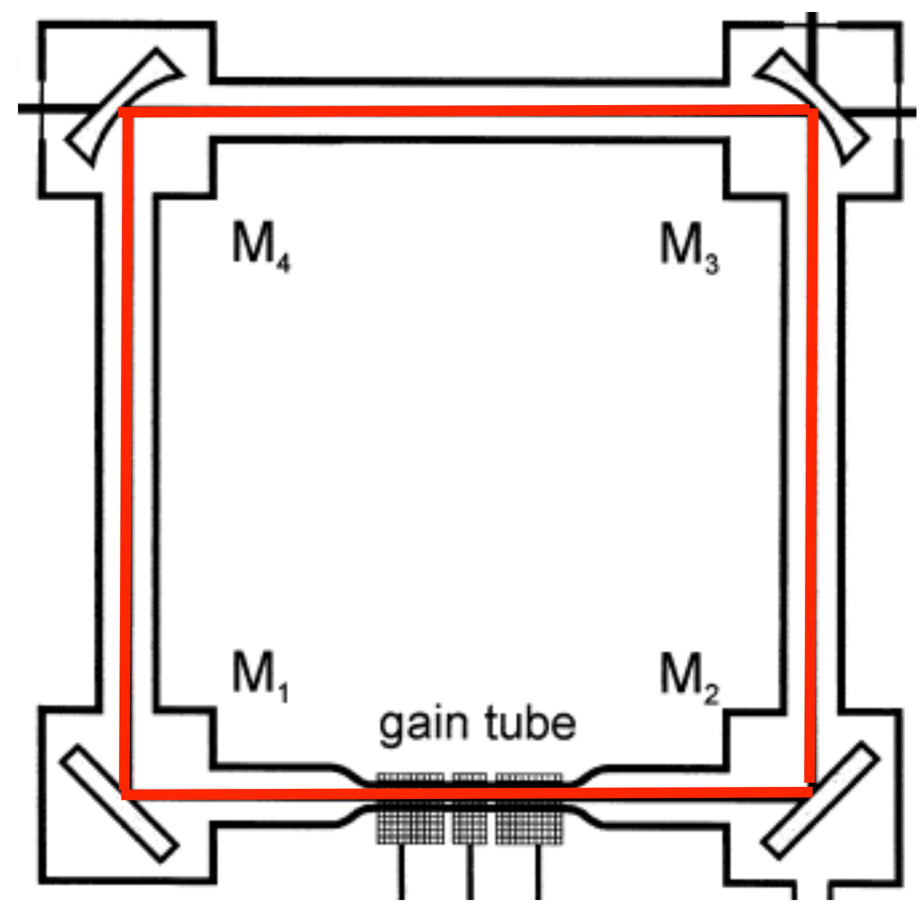

Relevant factors of influence

- scale factor
- rotation rate
- orientation
- nullshift error
- backscatter coupling

$$\delta f = \frac{4\,A}{\lambda\,P}\,\vec{n}\cdot\vec{\Omega} + f_{nr}$$

$10^{-9}\,\Omega_E \approx 0.07$ prad/s

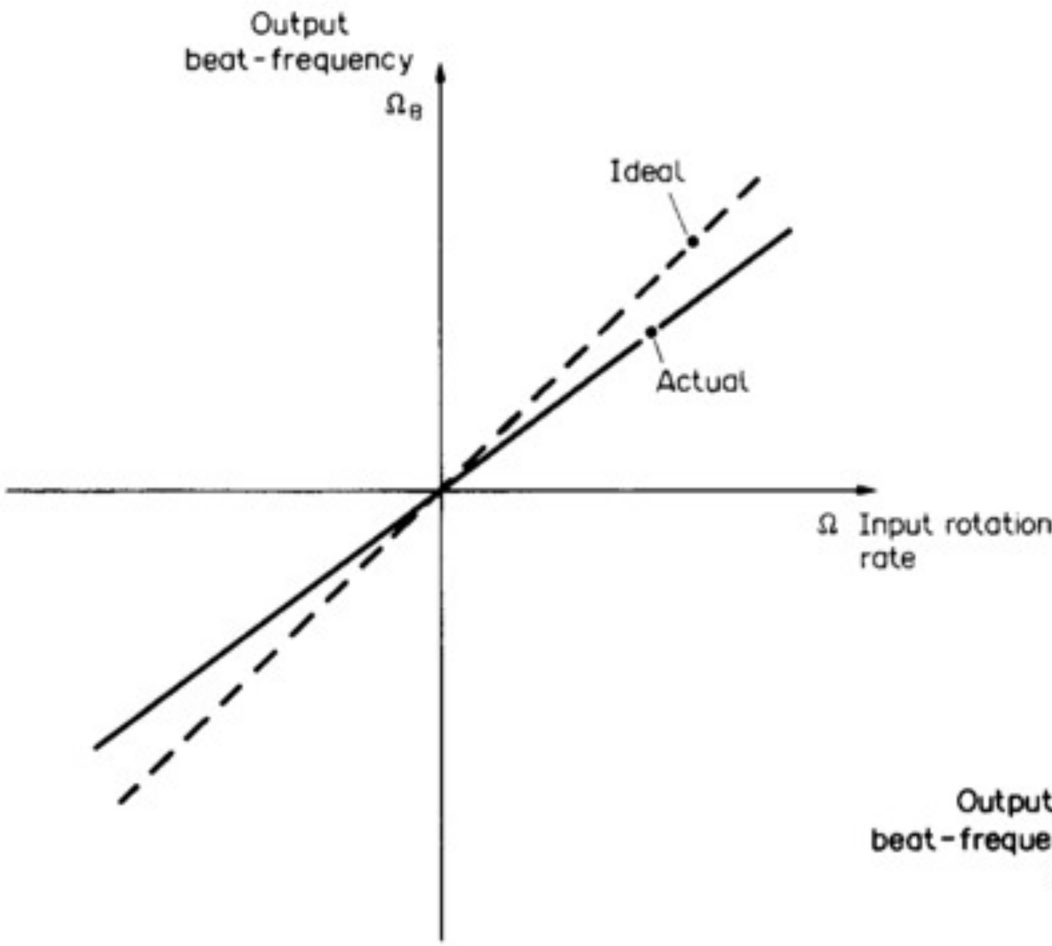

scale factor error

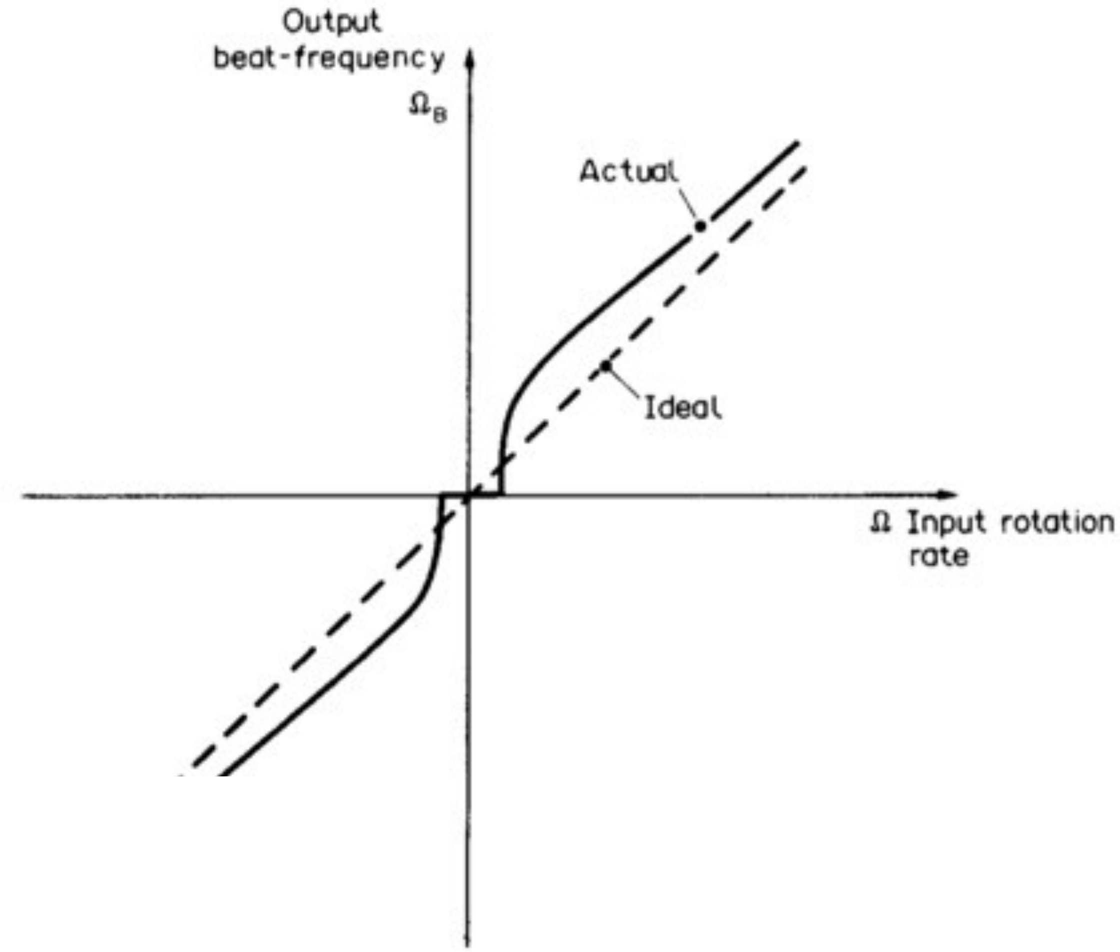

lock-in

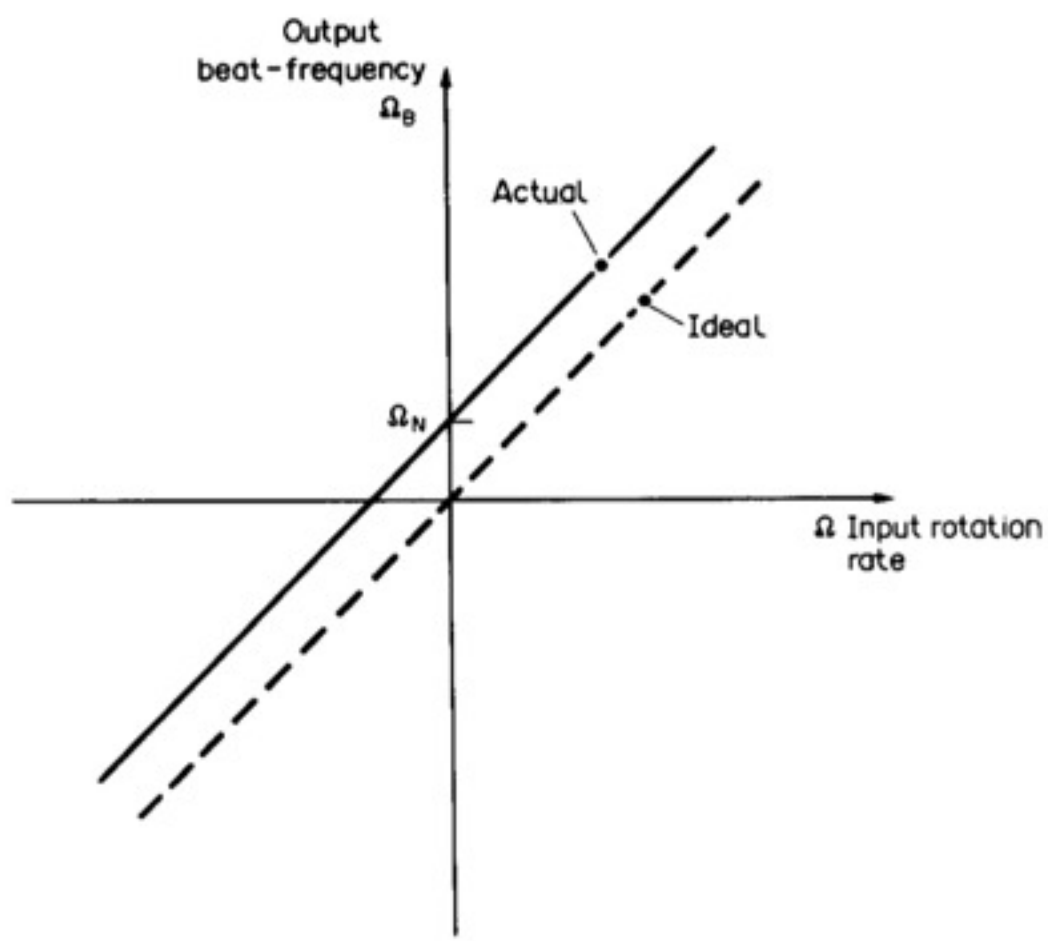

null shift error

Ring laser have a very large dynamic range and a transfer function of unity

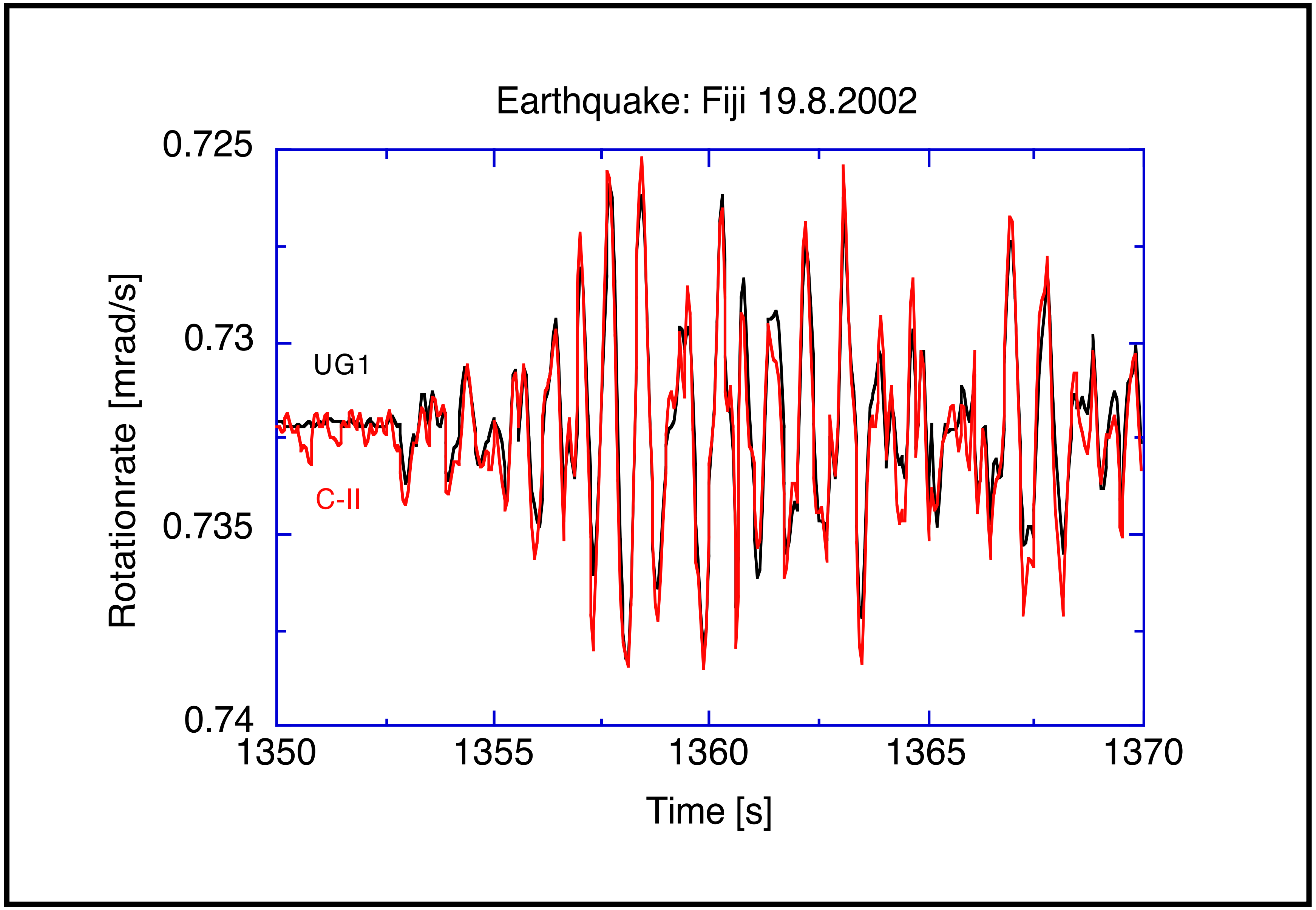

Scale Factor Variations in UG-2 inferred from Beam Wander Measurements

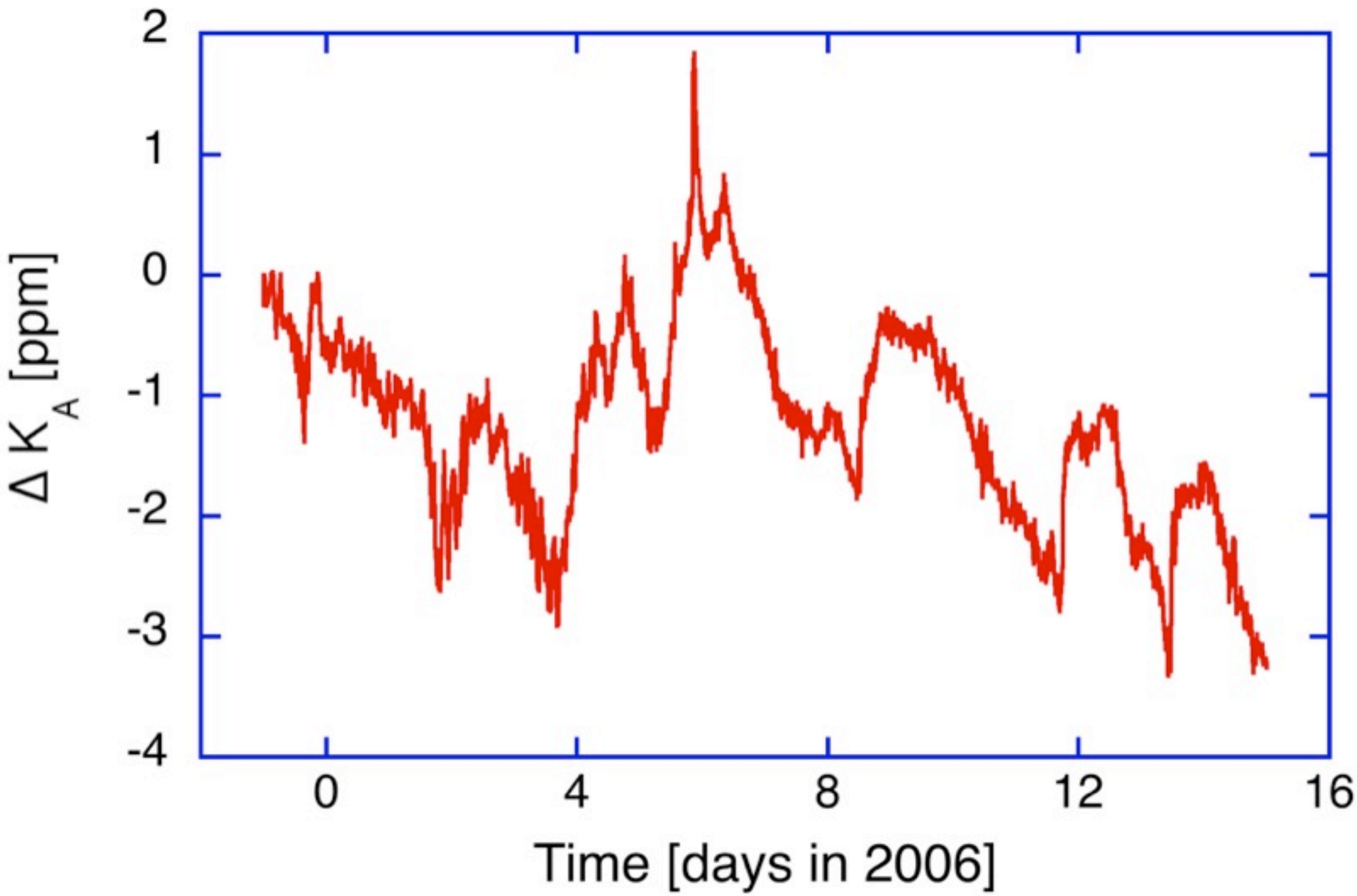

Lock-In Effect causes Biases

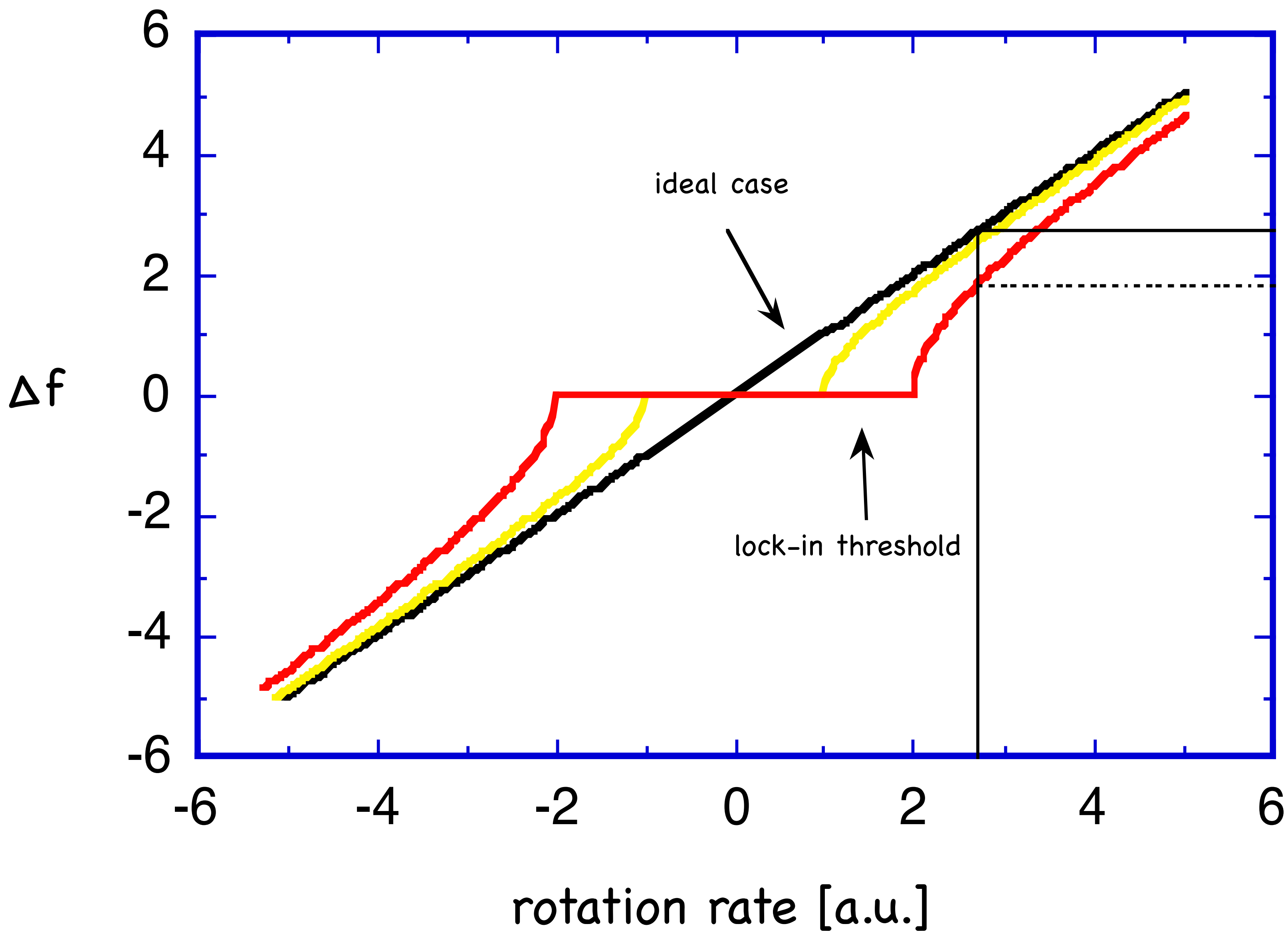

Since our ring lasers are large,the mirrors have low scatter losses and the instruments are strapped down to Earth, they can be taken as ideal sensors in the frequency window interesting in seismology.

This does no longer apply for strong motion

G - Ring @ Wettzell

- Perimeter: 16 m
- Area: 16 m^2
- FSR 18.75 MHz
- $\Delta \nu_L \approx 274\ \mu Hz$
- 5 ppm total loss
- $Q = \omega \tau \approx 5x10^{12}$
- 6.5 mB gas pressure in order to avoid multi-moding

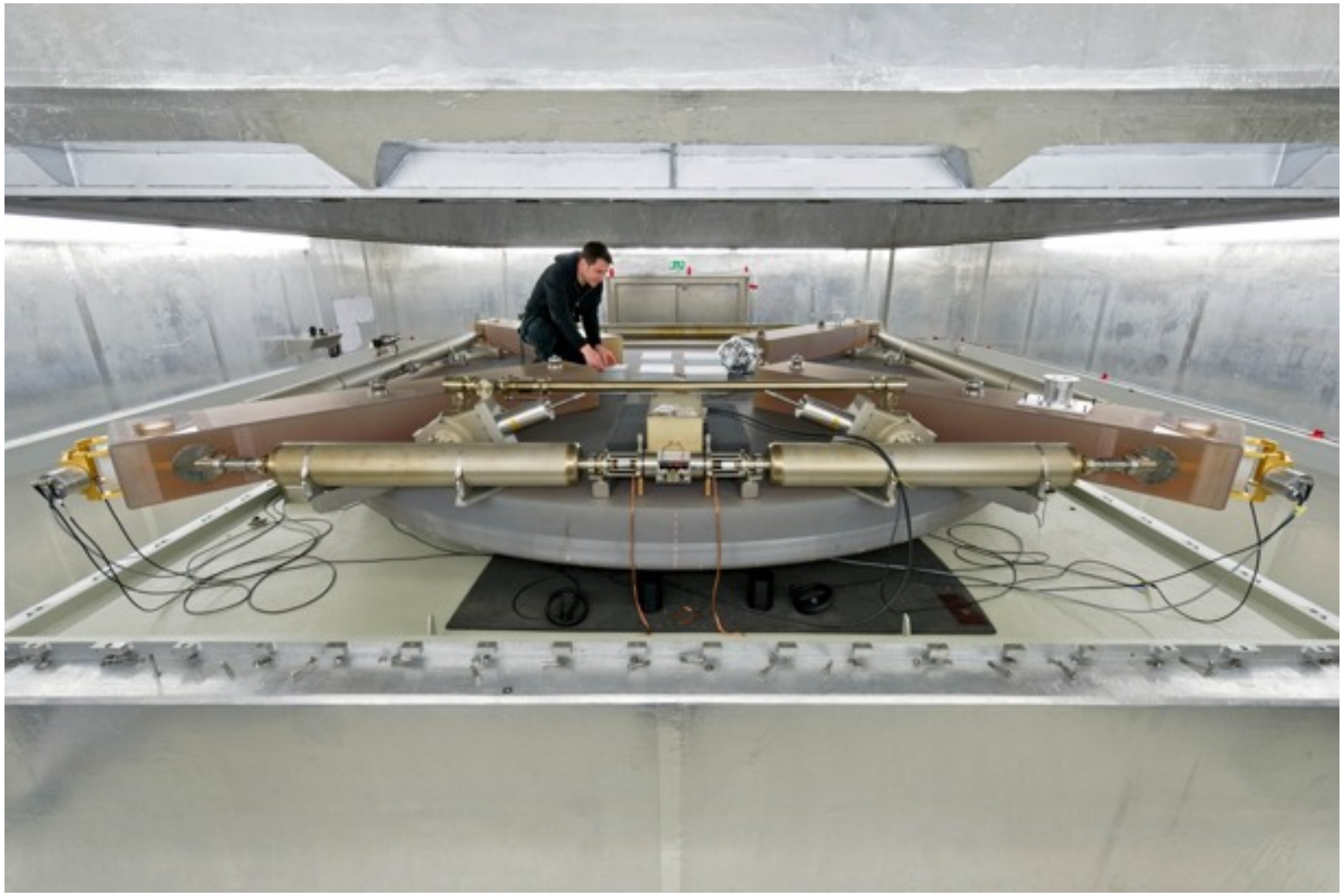

Geodetic Observatory Wettzell

A ring laser structure, which is rigidly attached to the body of the Earth, can be viewed as a highly stable clock oscillator, whose tiny variations...

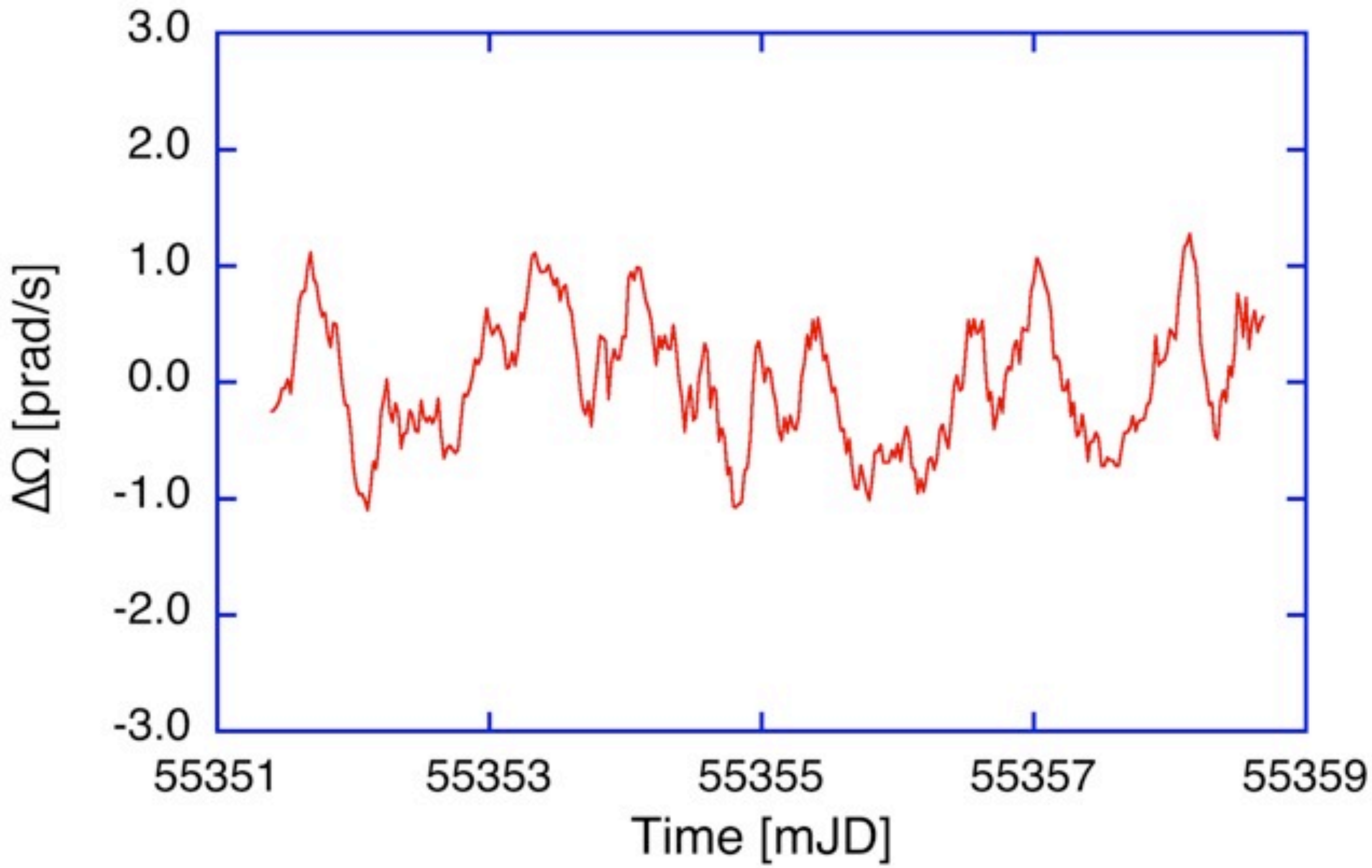

... are a result of global processes

stability assessment per Allan deviation

$$\sigma^2 = \frac{1}{2\,(n-1)} \sum_{i=1}^{n-1} (\nu_{i+1} - \nu_i)^2$$

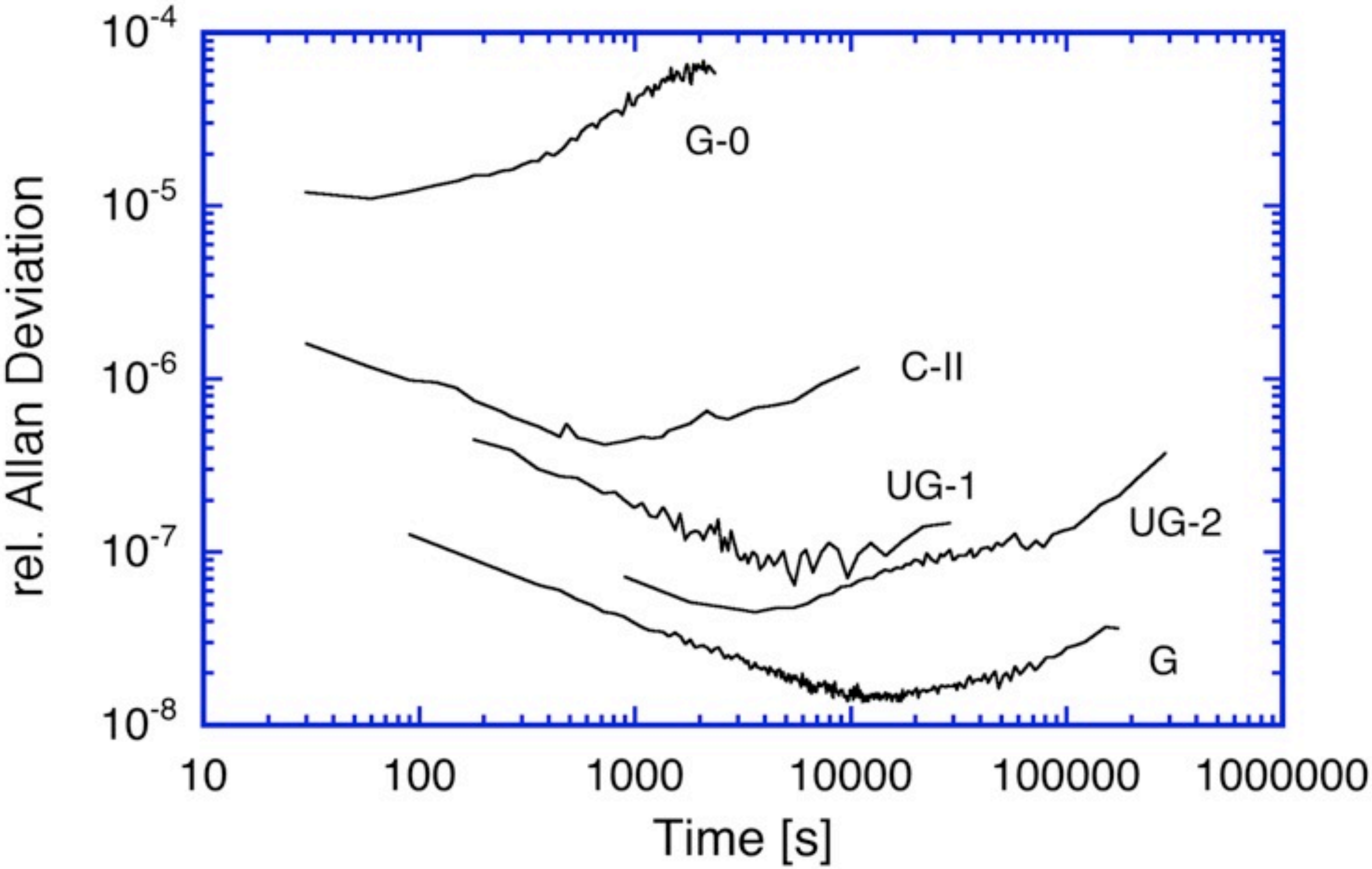

Effects of changing orientation on a ring laser

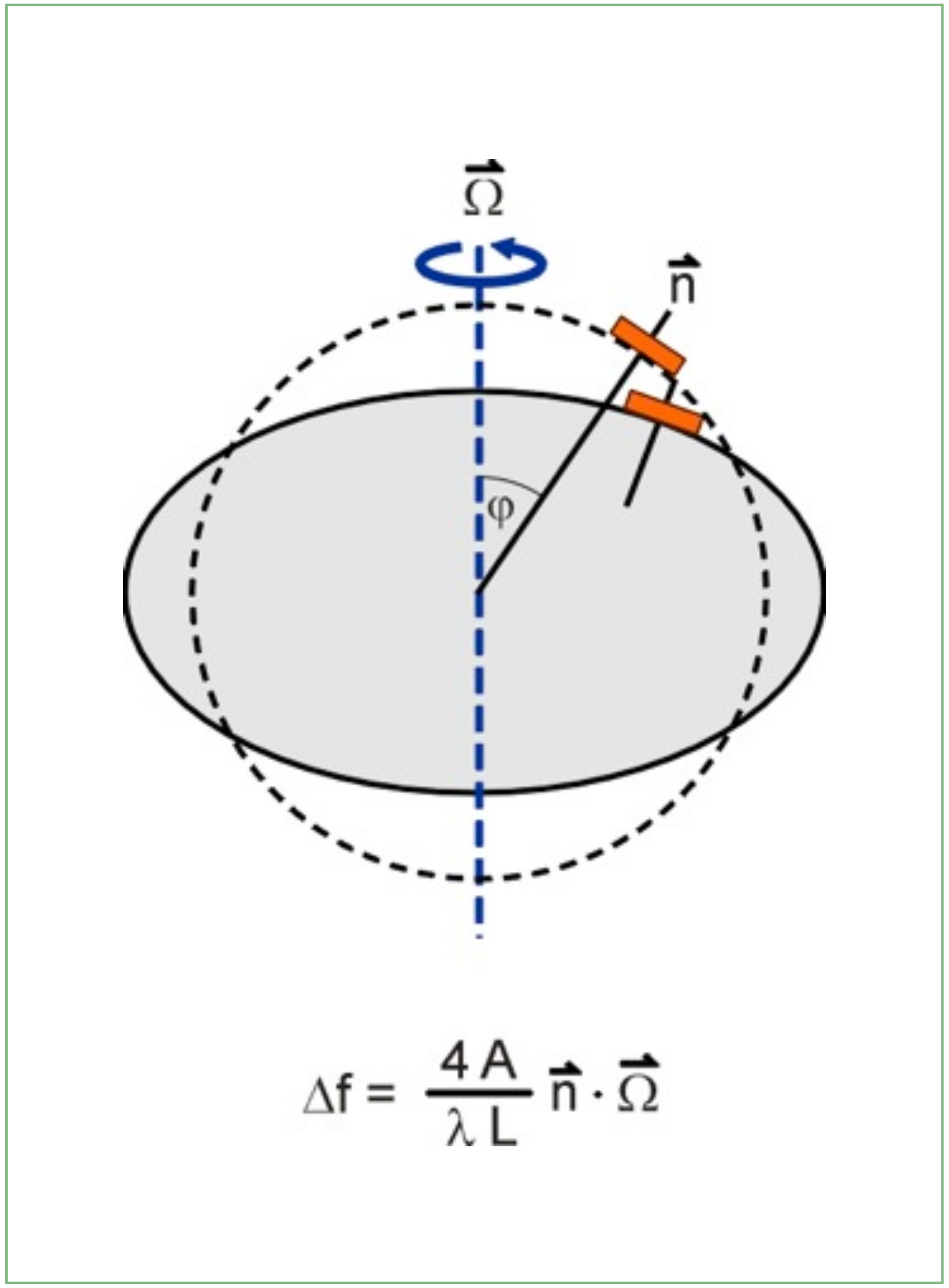

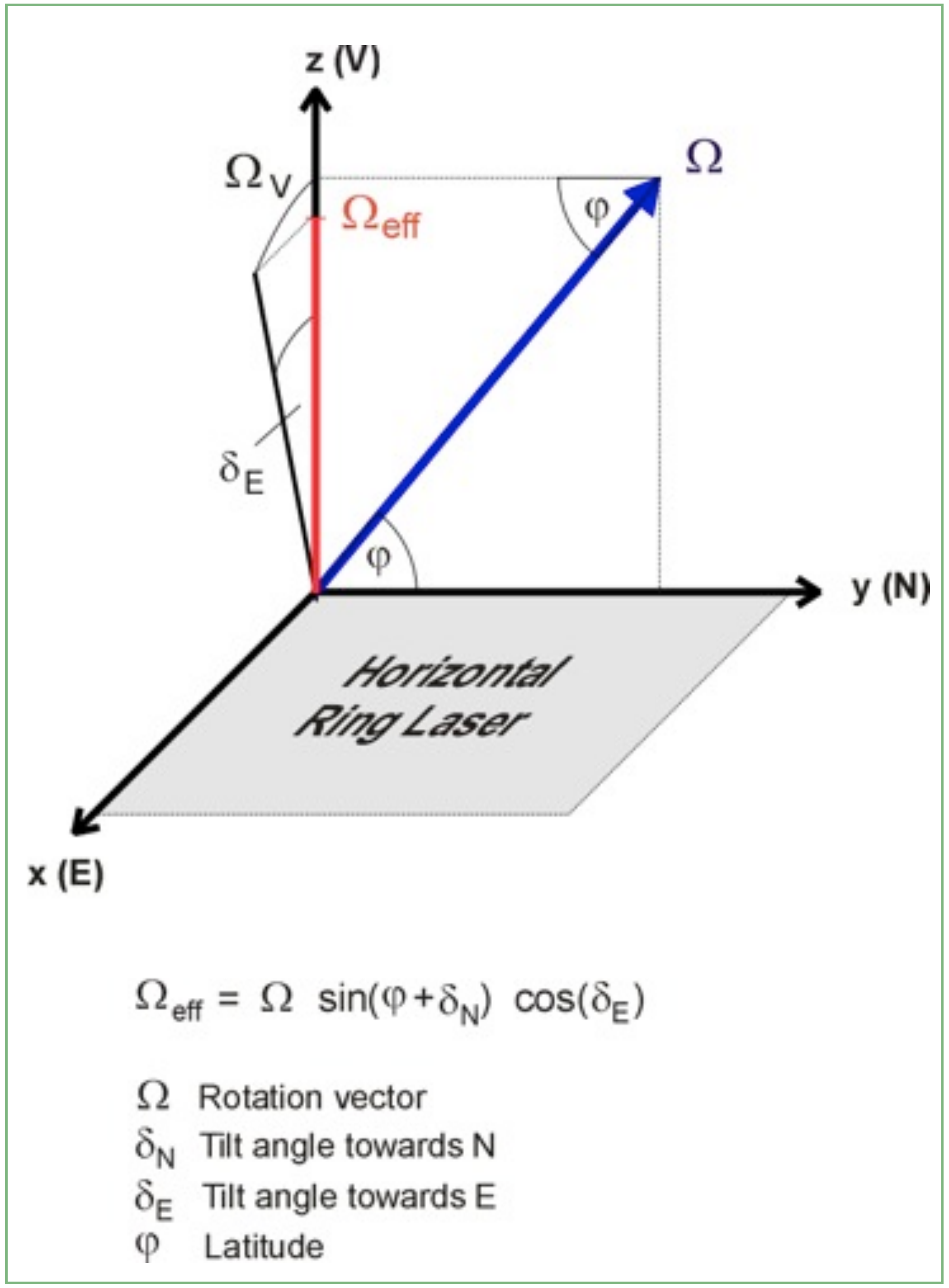

Effects of changing orientation on a ring laser

Measurements compared to the models

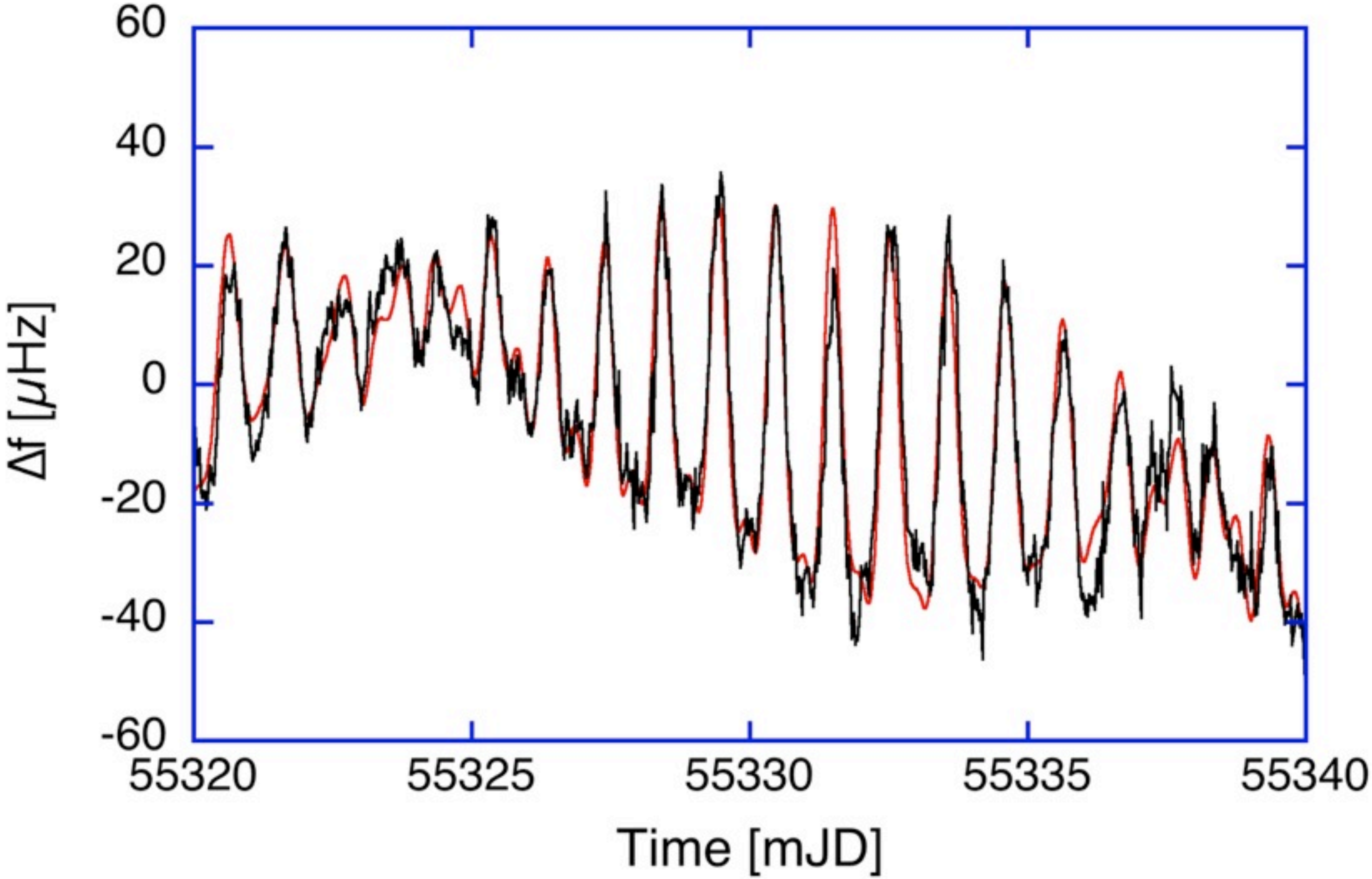

… the Chandler and the annual wobble

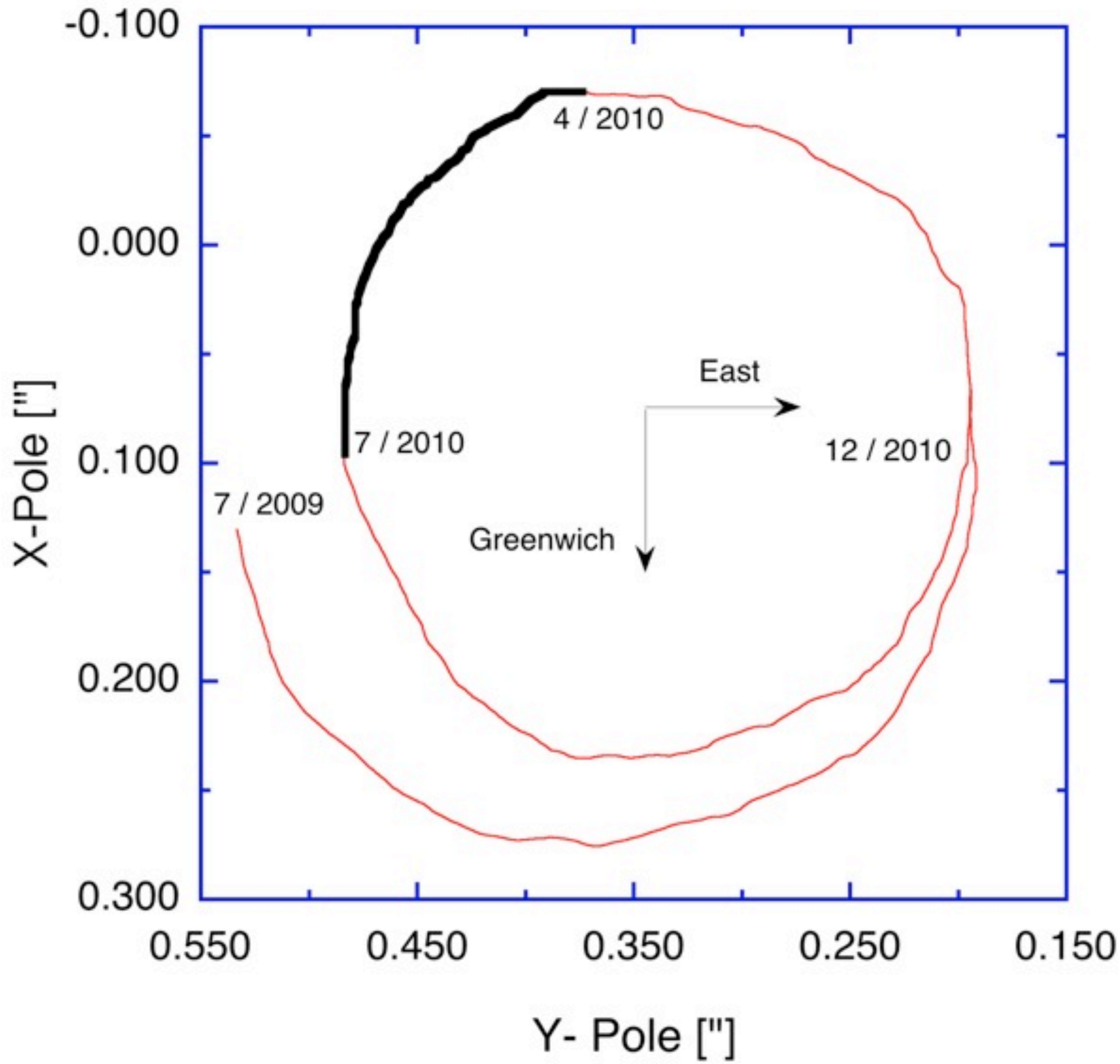

Comparison to VLBI measurements

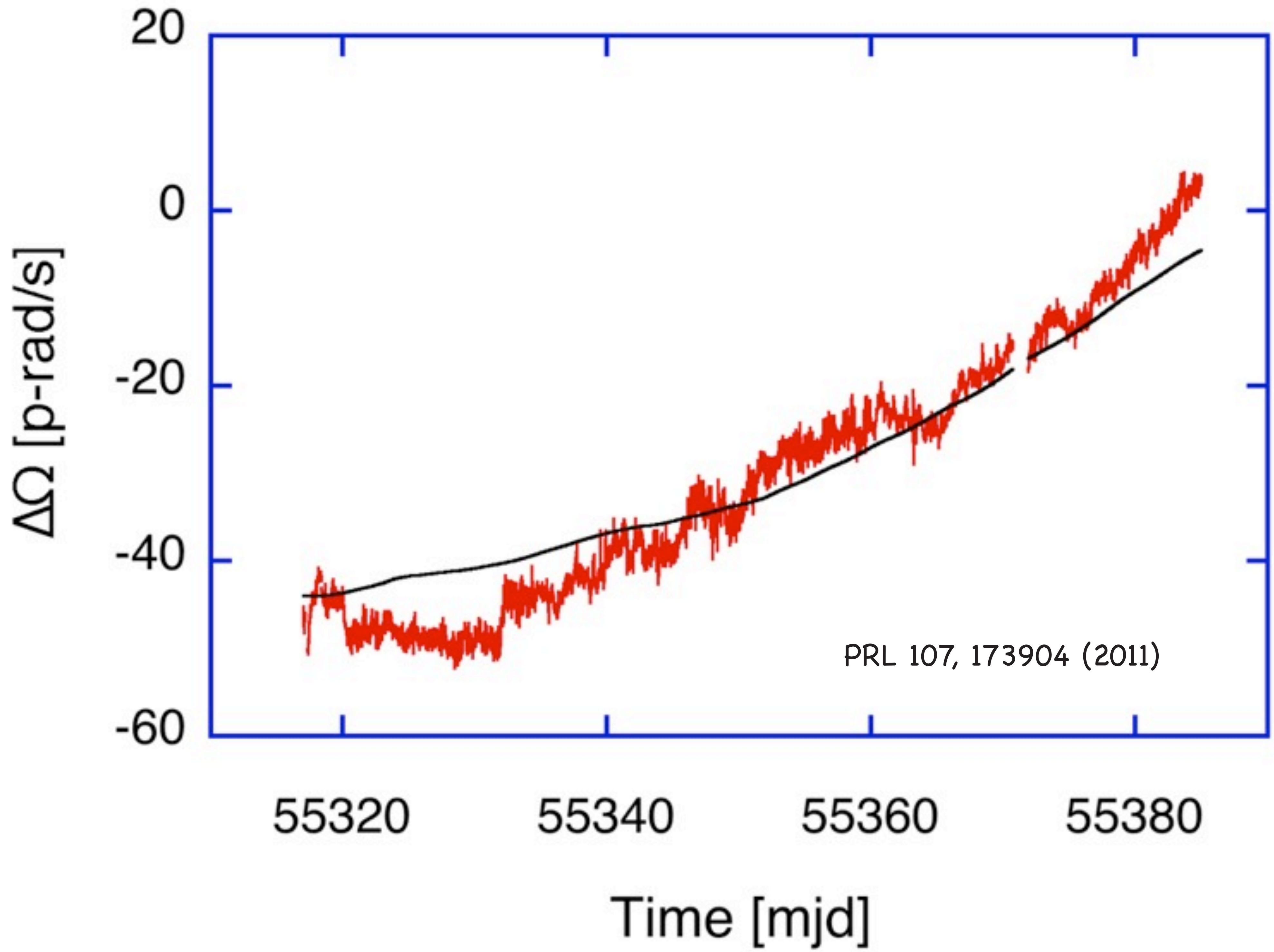

Variations in ambient pressure change the scale factor, but more so the phase of the backscatter signal. The optical frequency is shifting by 330 kHz per hPa.

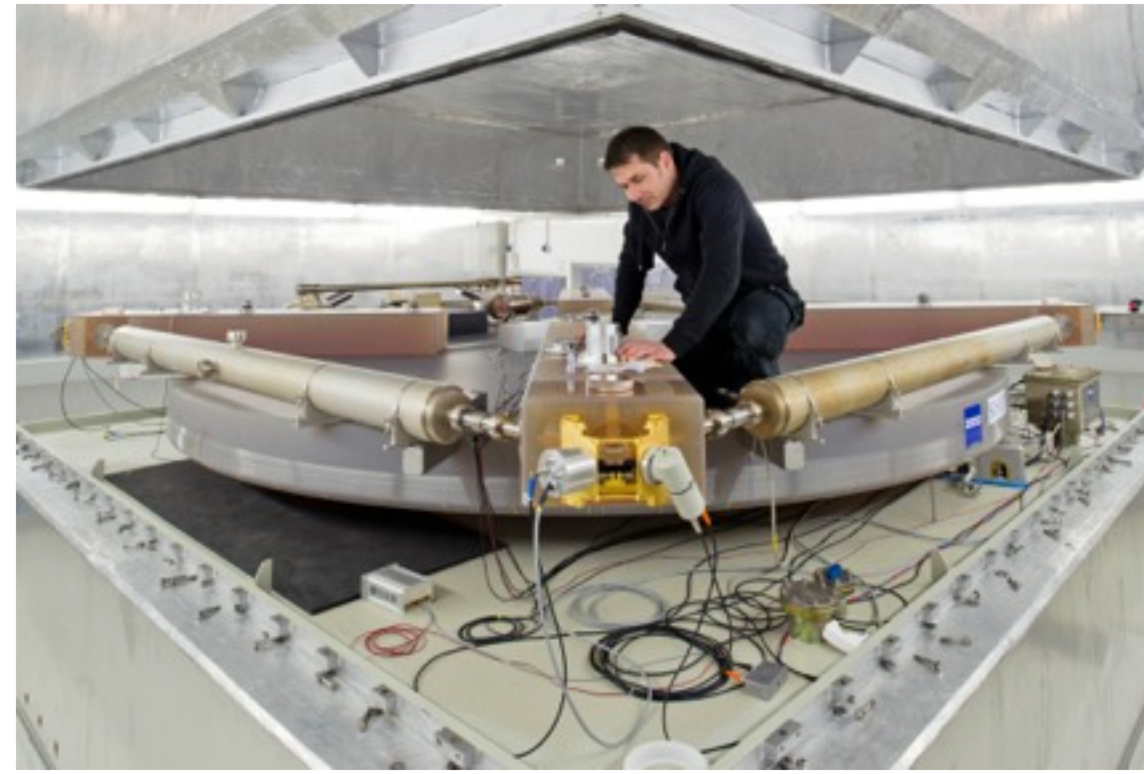

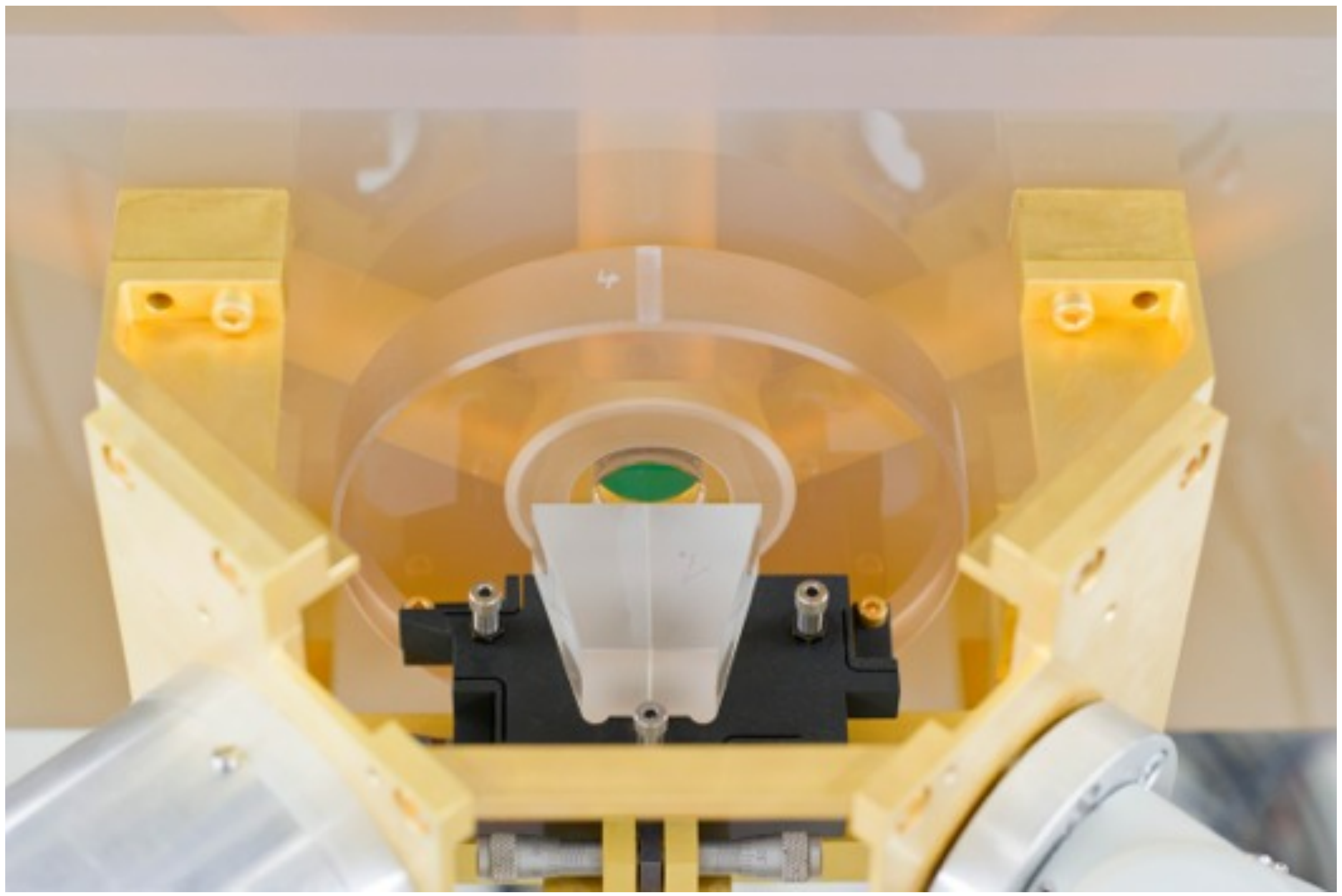

Using a pressure stabilizing vessel (developed together with UoC) the drift of the optical frequency in the cavity could be significantly reduced…

… this caused most notably a substantial reduction of backscatter variation.

Backscatter induced instability of the interferogram.

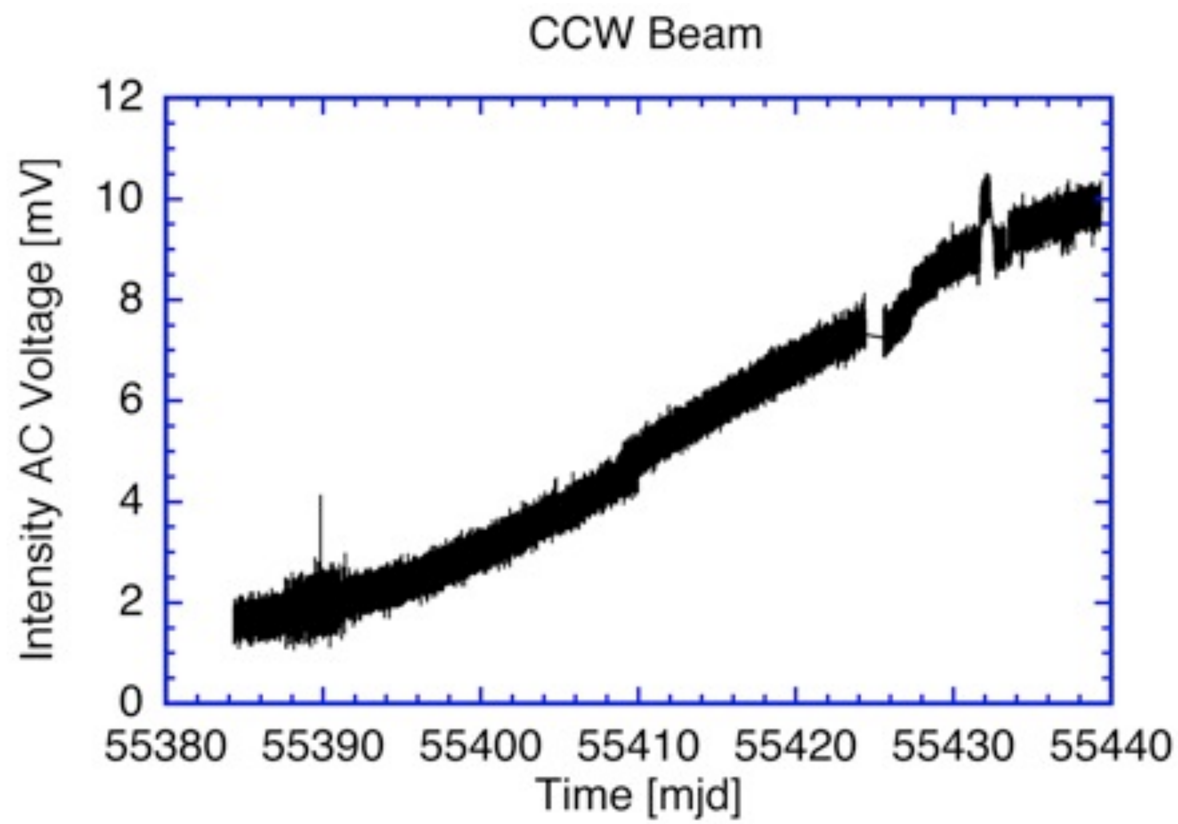

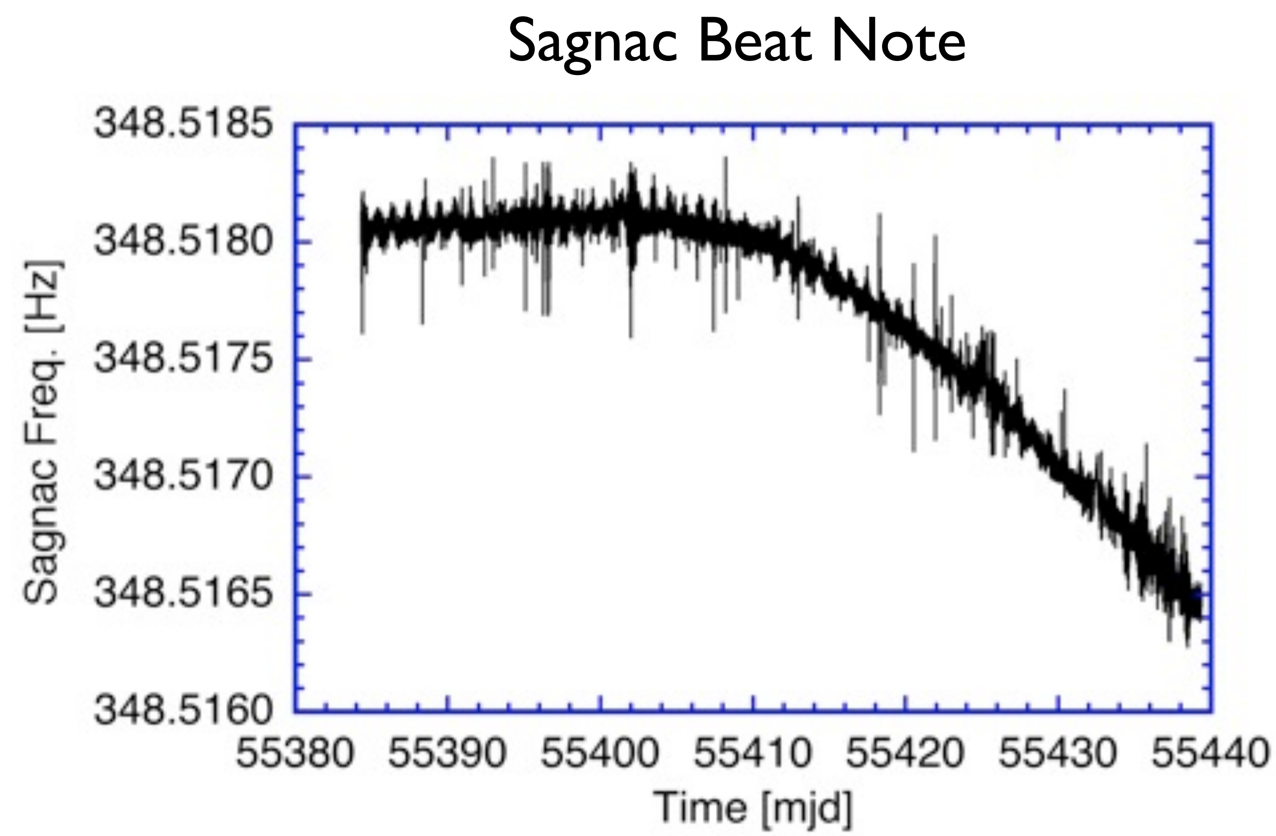

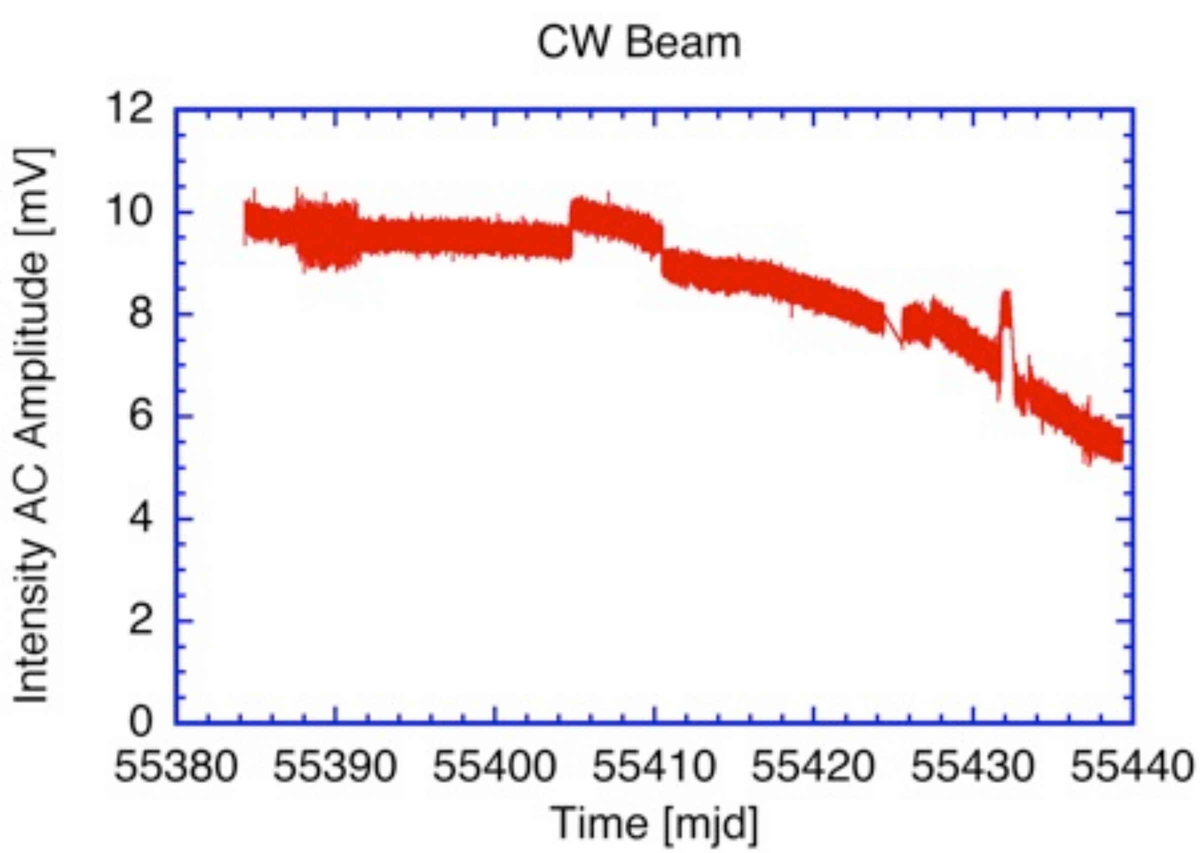

Monobeam Intensities filtered @ 348 Hz and Peak - Peak Amplitudes estimated

Nullshift Stabilization

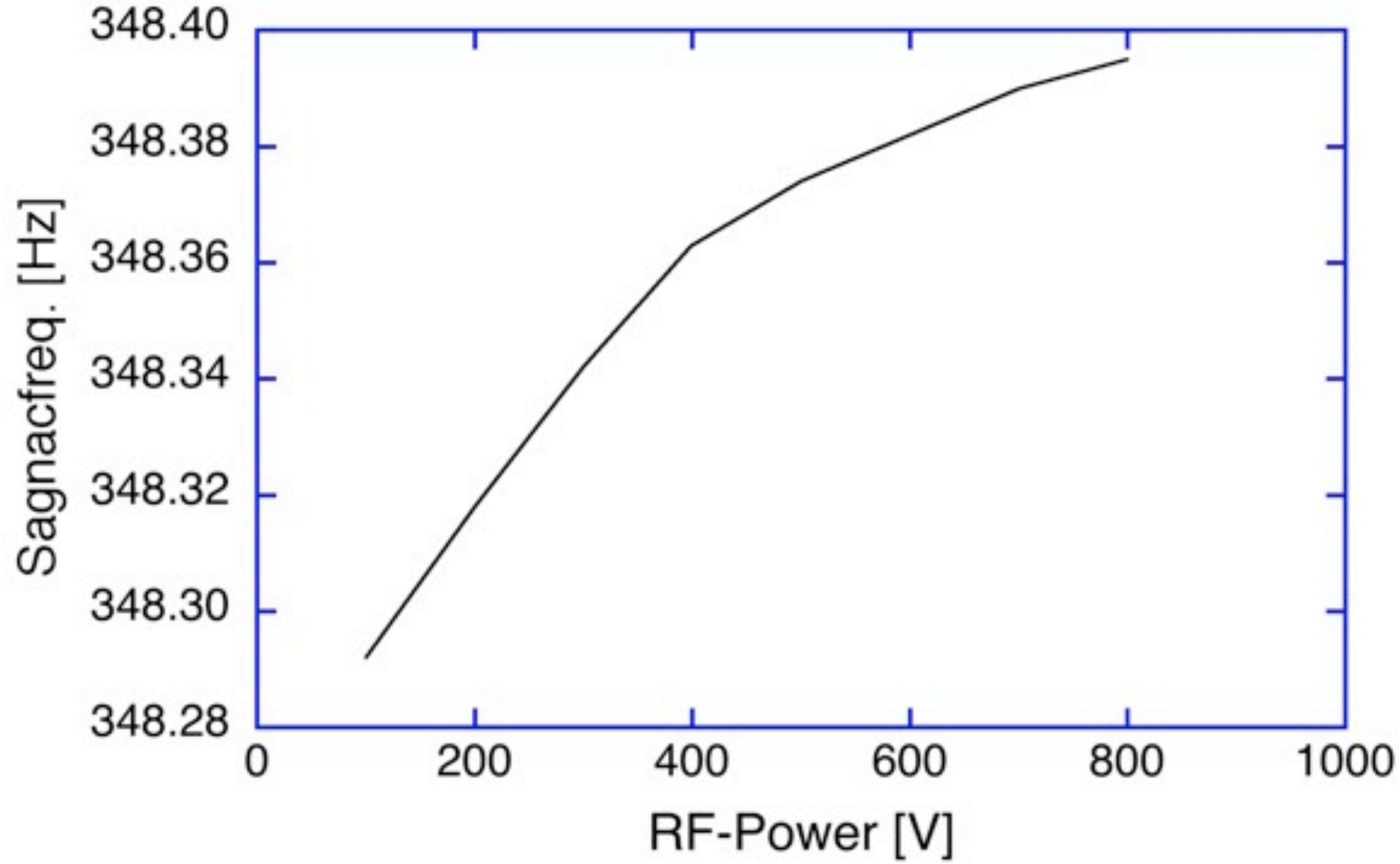

ALL of our rings exhibit an asymmetry with respect to the effective Q factor of the cavity per sense of propagation, which results in a offset value depending on the brightness of the laser beam. For G the difference in brightness is about 1%.

A feedback circuit stabilizes the brightness and hence the point of operation (< 0.1%).

Interim Summary:

$$\delta\Omega = \frac{cP}{4AQ}\sqrt{\frac{hf}{P_x t}}; \qquad \delta\Omega = 1.2\times10^{-11}\,\frac{\text{rad}}{\text{s}\sqrt{\text{Hz}}}$$

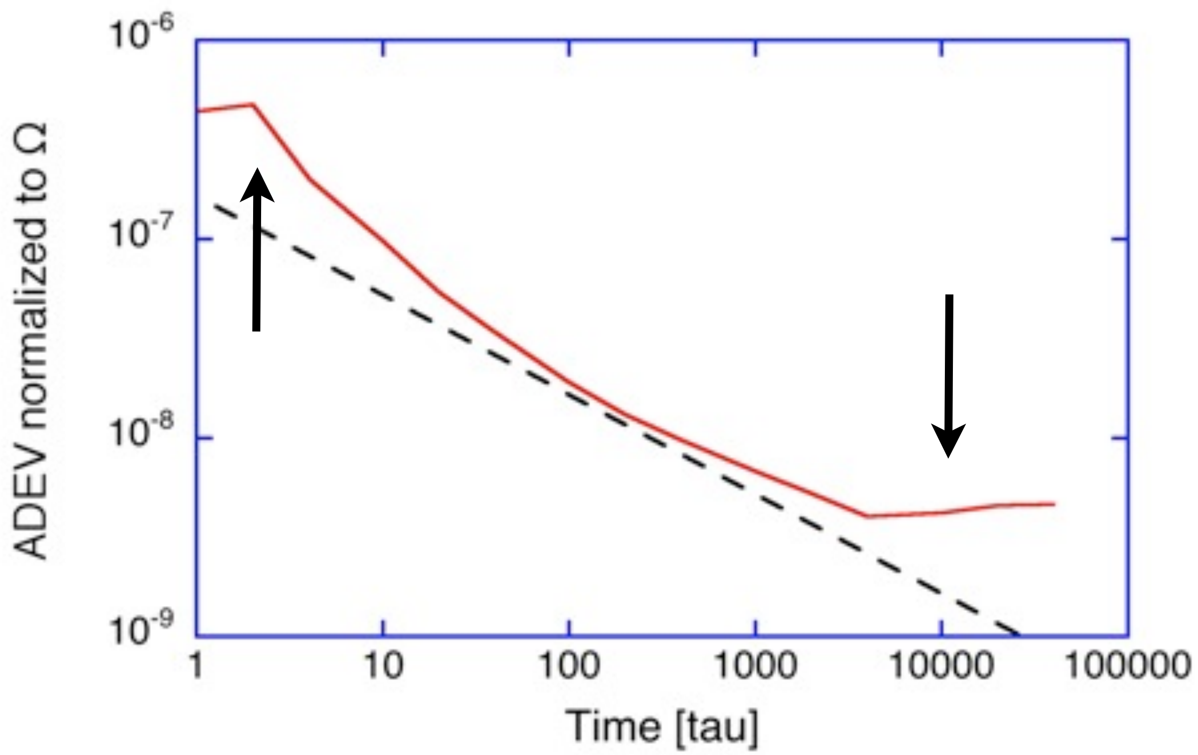

- Sensitivity sufficient
- limited by micro seismics for short integration times (signal!)
- limited by stability for long integration times (backscatter)

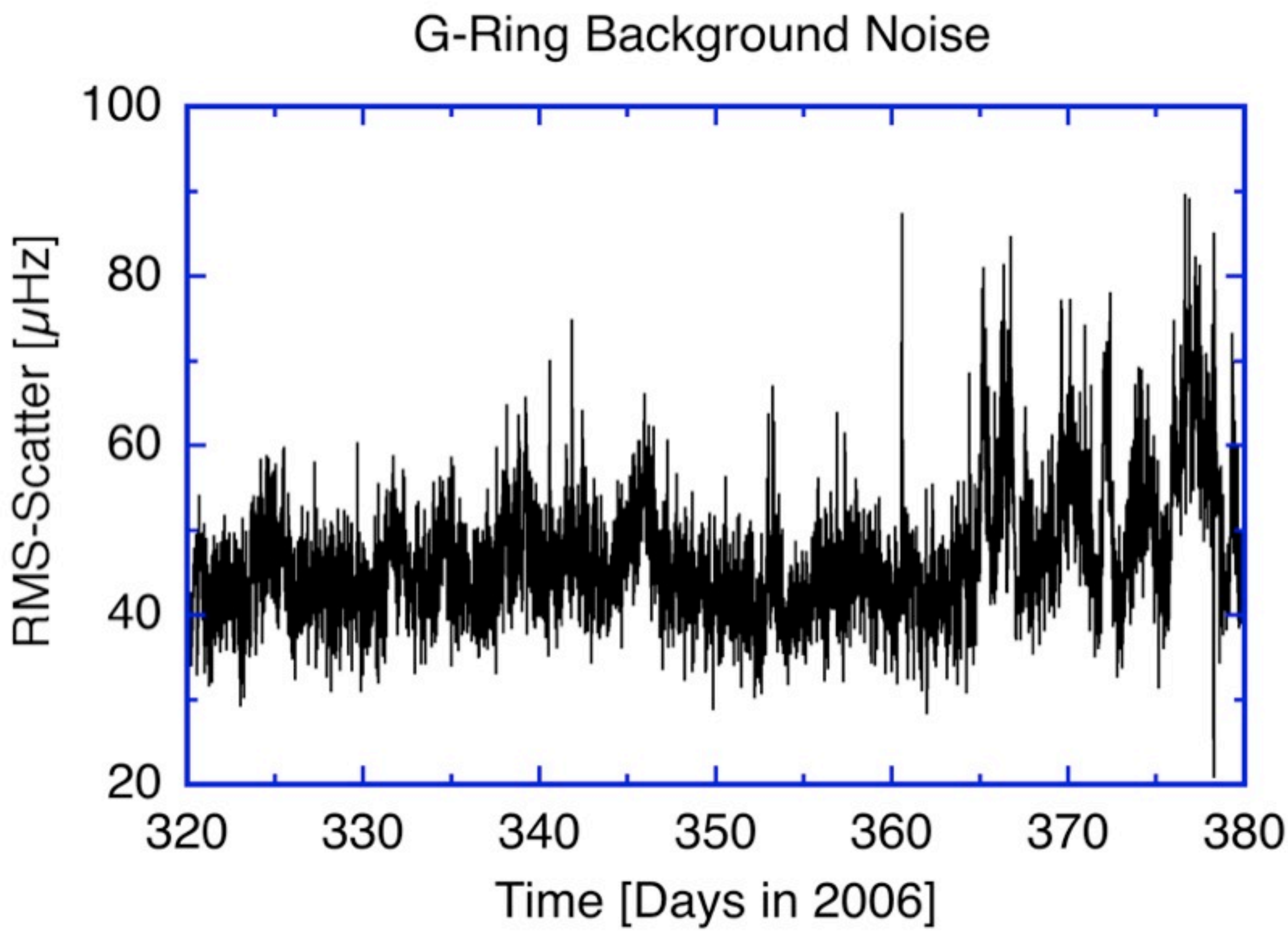

G-Ring Background Noise
RMS-Scatter [μHz]
Time [Days in 2006]
100
80
60
40
20
320
330
340
350
360
370
380

applied changes:
ULE substrates -> fused Silica substrates

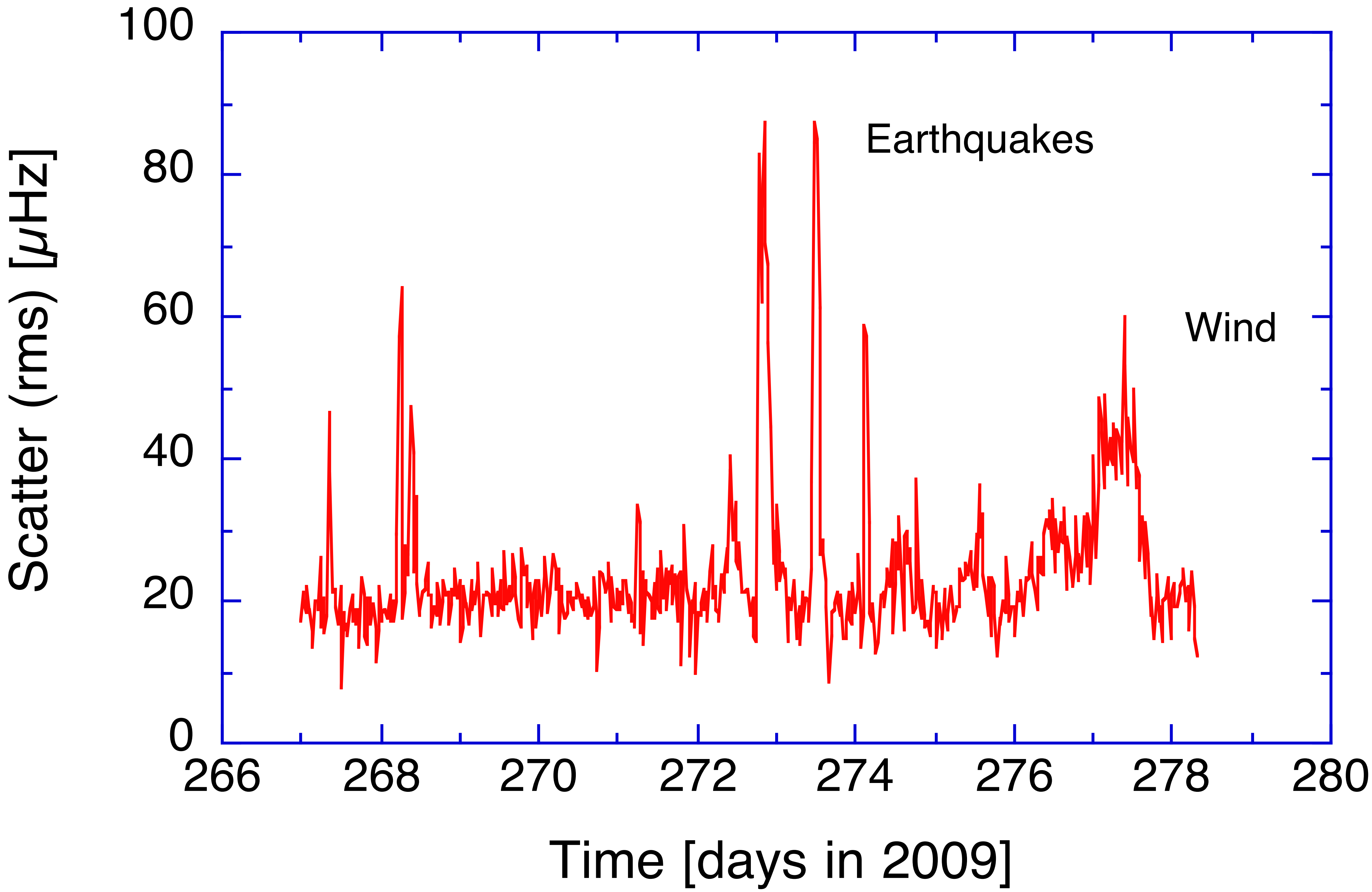

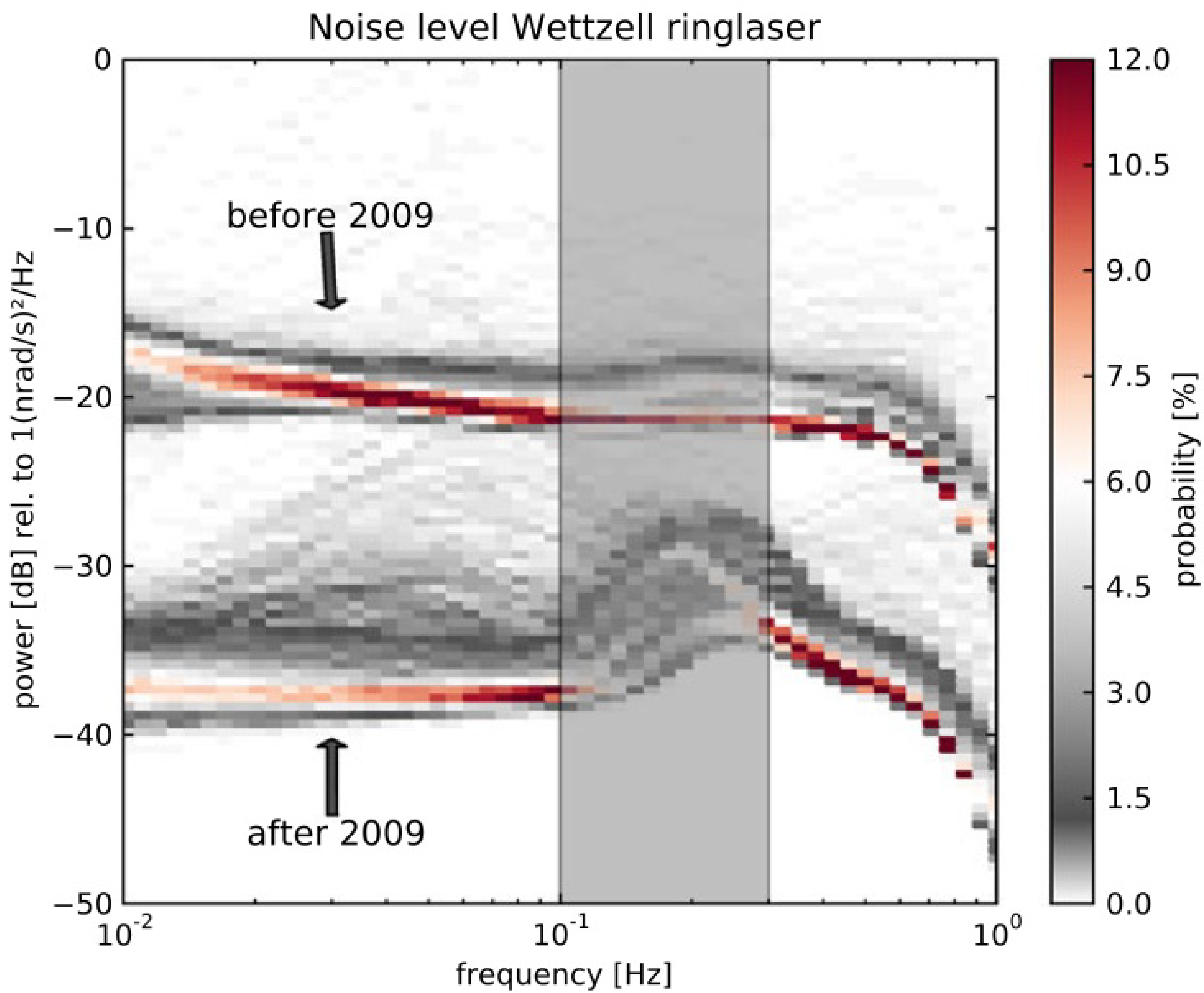
Noise level Wettzell ringlaser
0
−10
−20
−30
−40
−50
power [dB] rel. to 1(nrad/s)²/Hz
before 2009
after 2009
10^-2
10^-1
10^0
frequency [Hz]
12.0
10.5
9.0
7.5
6.0
4.5
3.0
1.5
0.0
probability [%]

Installation of the GEOsensor in Piñon Flat (CA, USA)

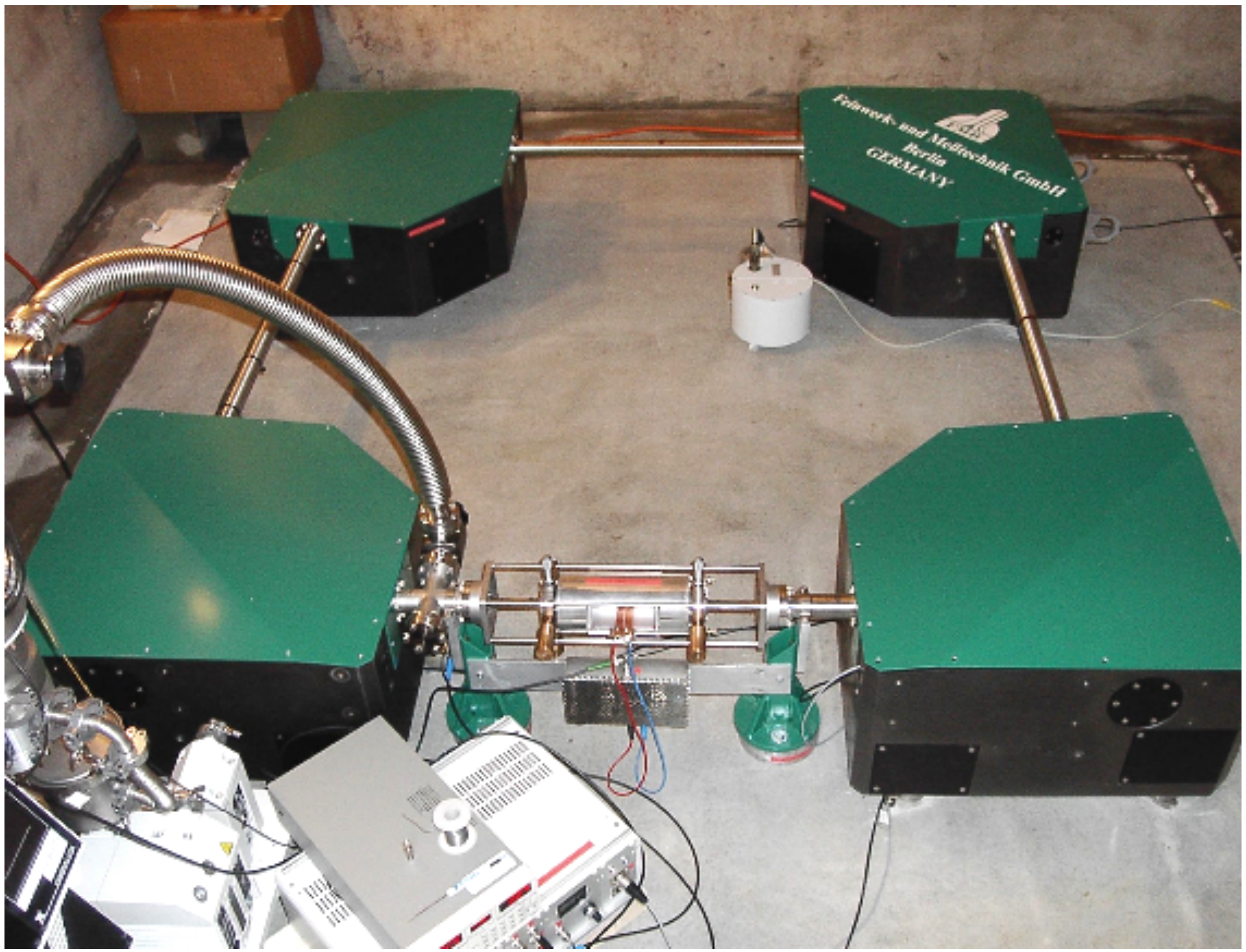

PFO Jan. 2005

Heterolithic Structure…

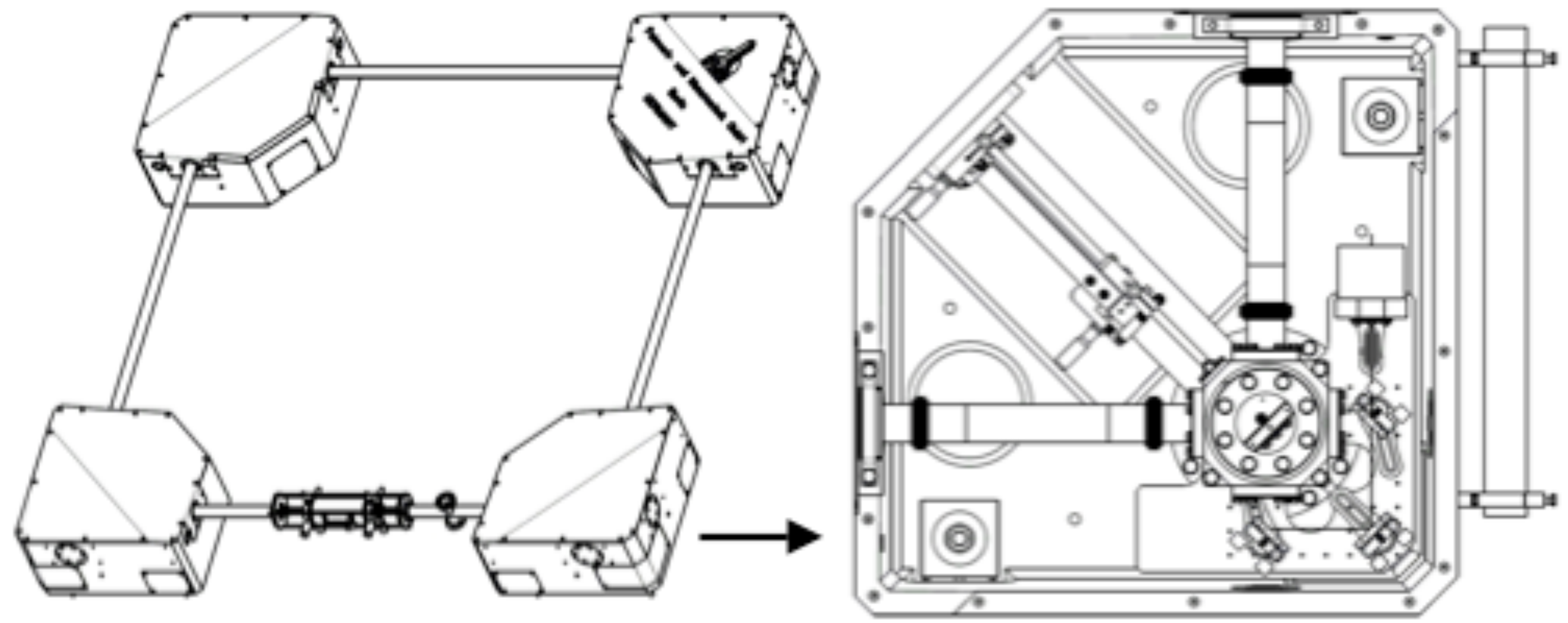

…requires active control

Modehops due to lacking stability

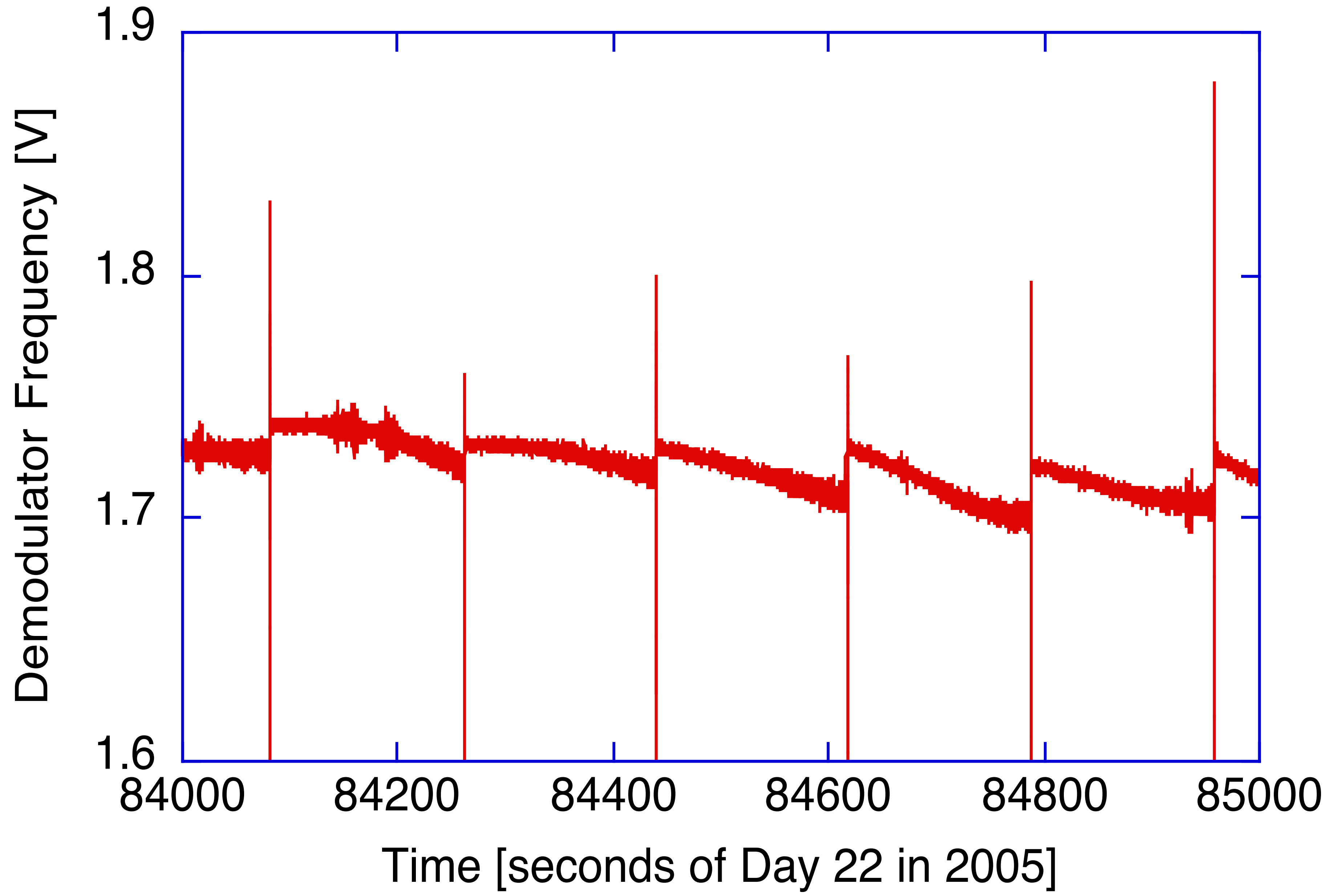

Splitmode!

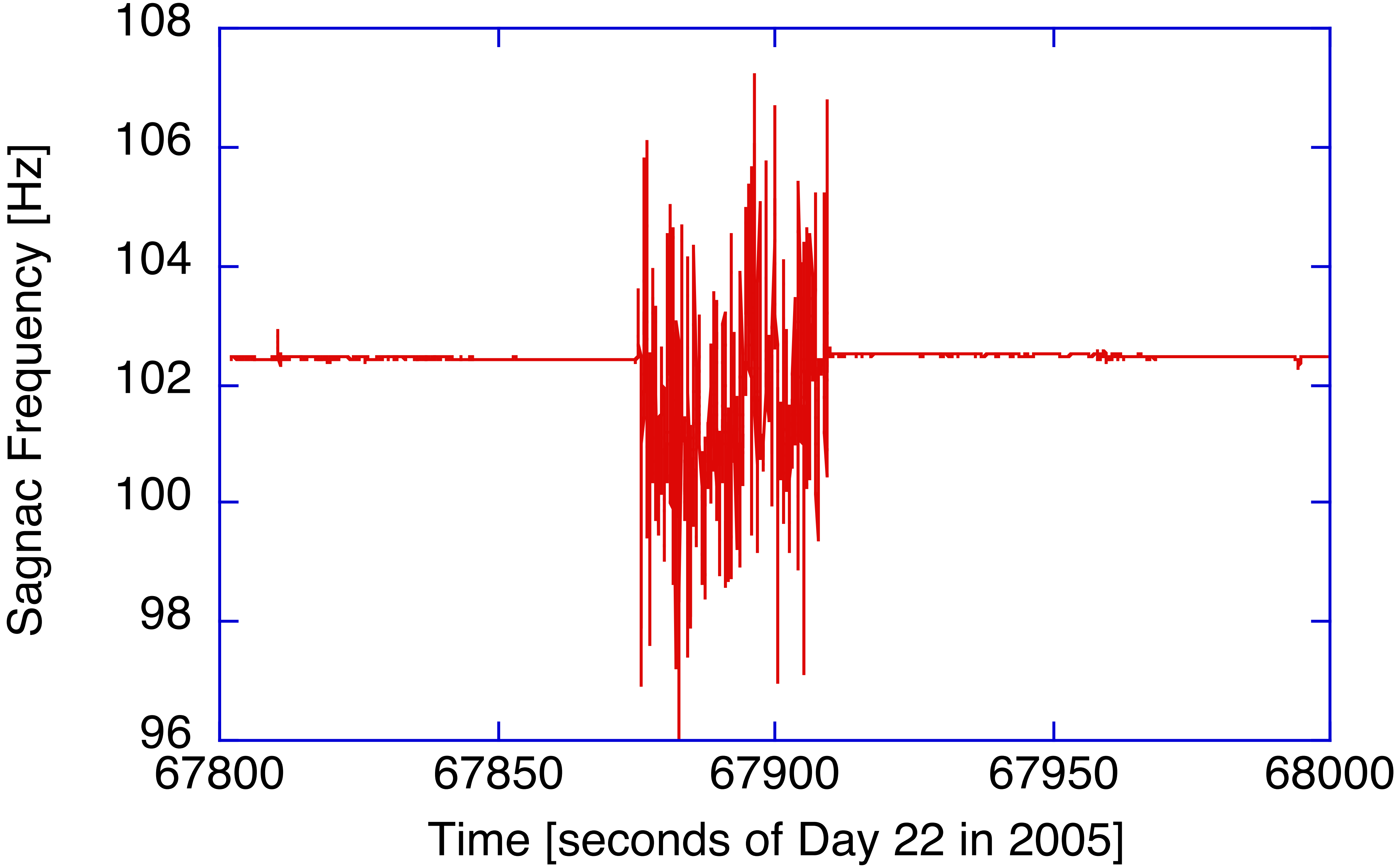
108
106
104
102
100
98
96
Sagnac Frequency [Hz]
67800
67850
67900
67950
68000
Time [seconds of Day 22 in 2005]

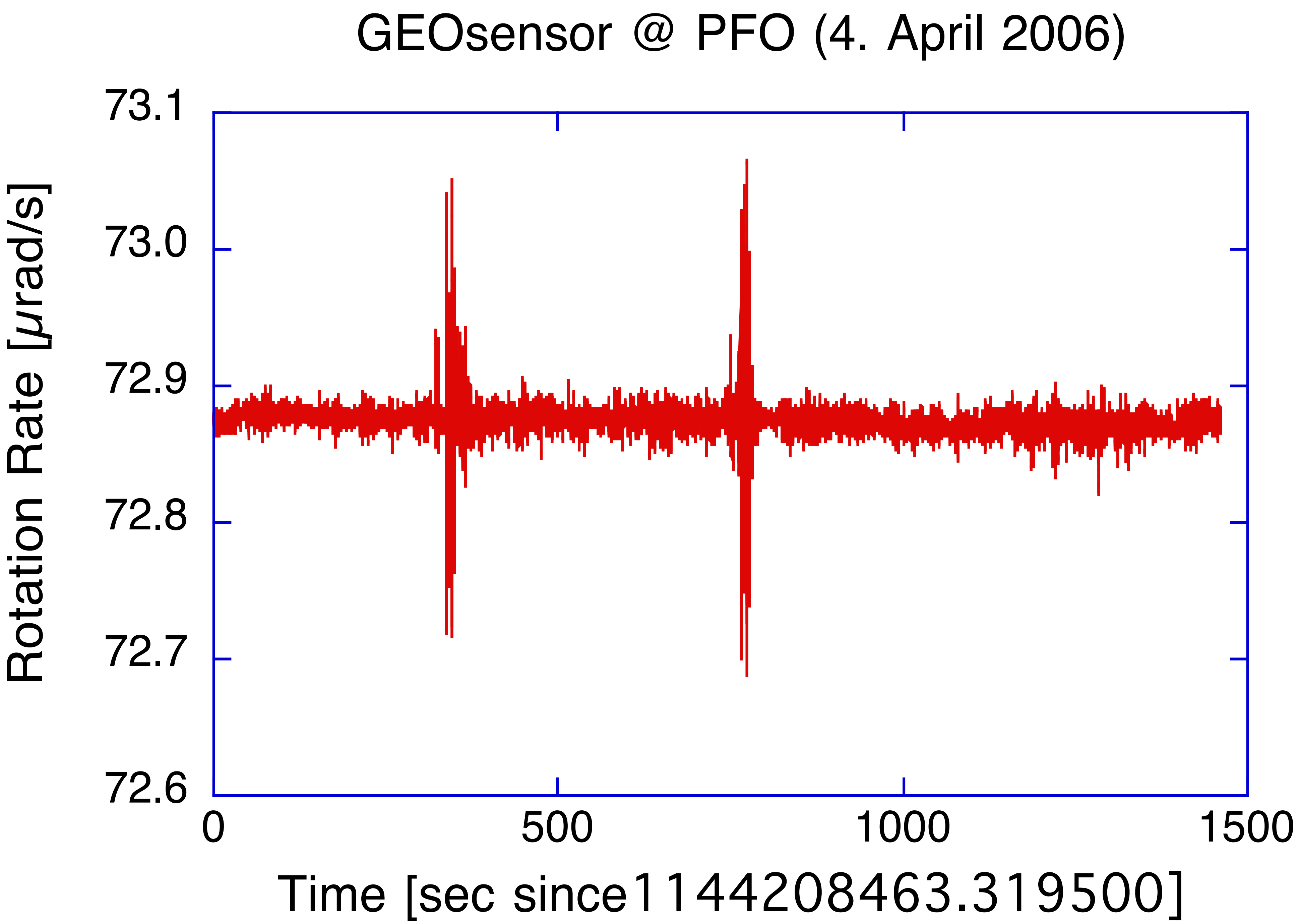
GEOsensor @ PFO (4. April 2006)
Rotation Rate [μrad/s]
73.1
73.0
72.9
72.8
72.7
72.6
0
500
1000
1500
Time [sec since1144208463.319500]

Improvements over the years

Active Perimeter and
Arm Control

Getter Functions

Higher Sampling

Different mirrors
(fused silica option open)

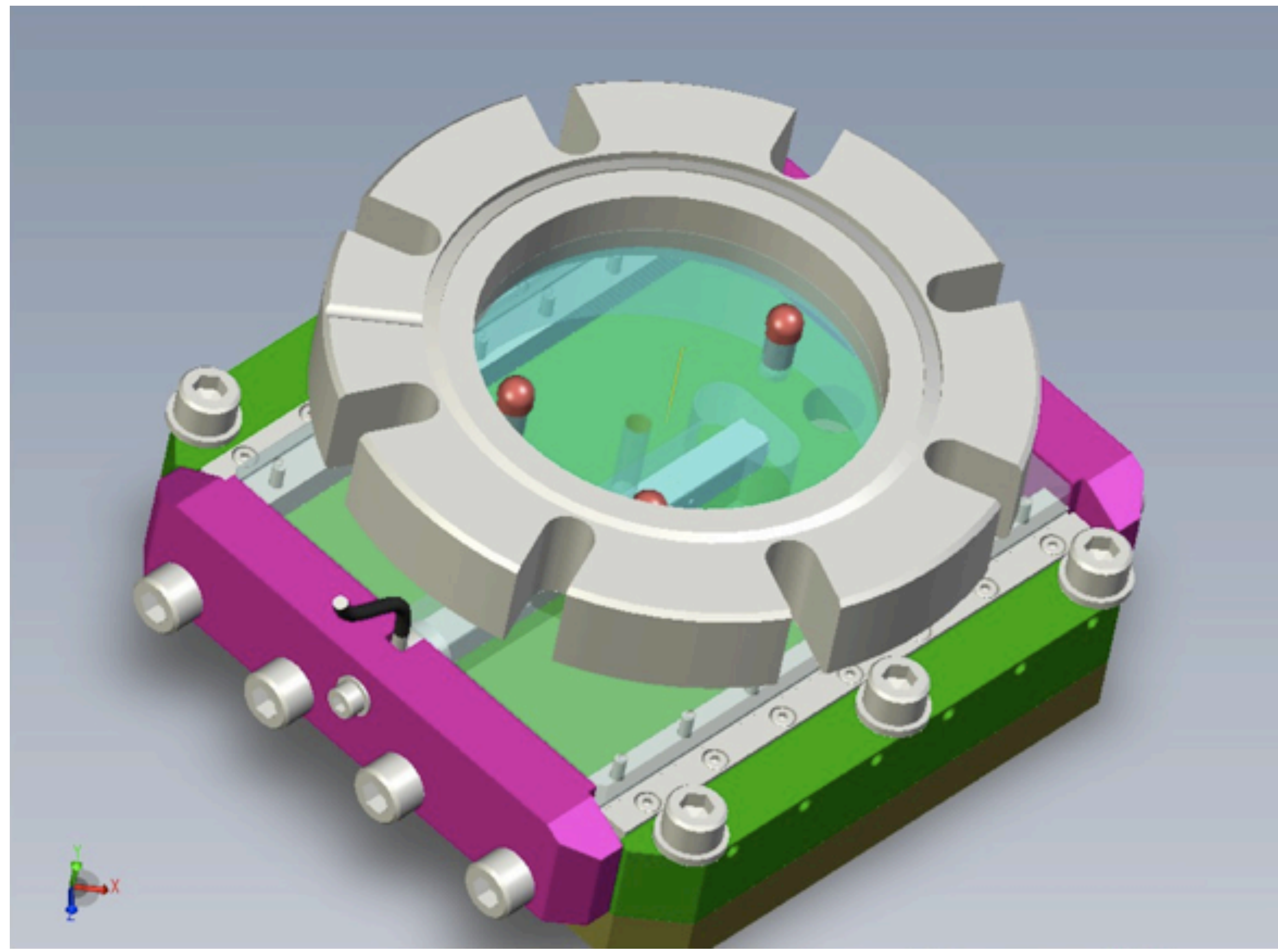

Data logging within the extended realtime Network

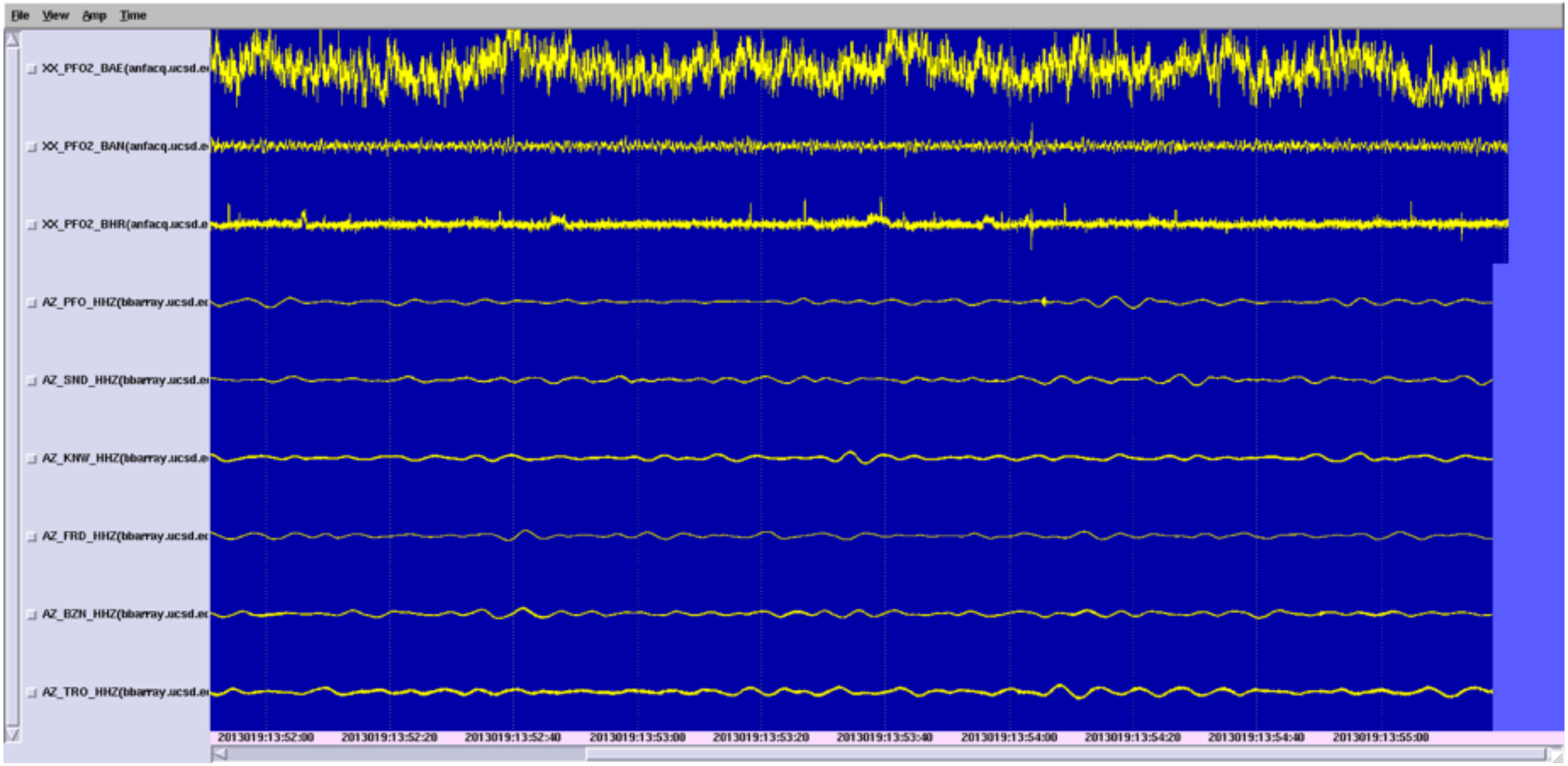

Current Activity -> opt. Frequency Stabilization

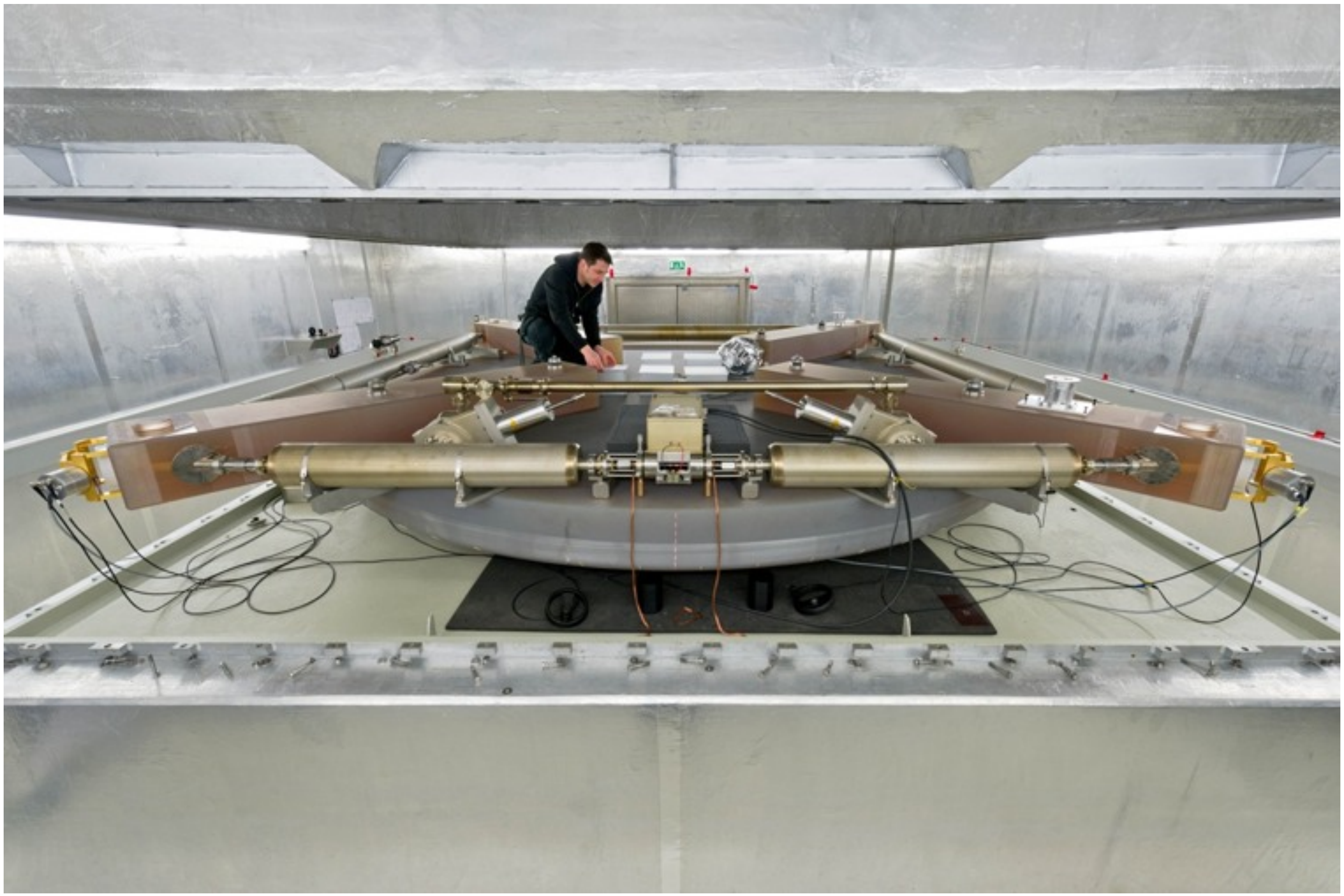

Remaining signature on the interferogram

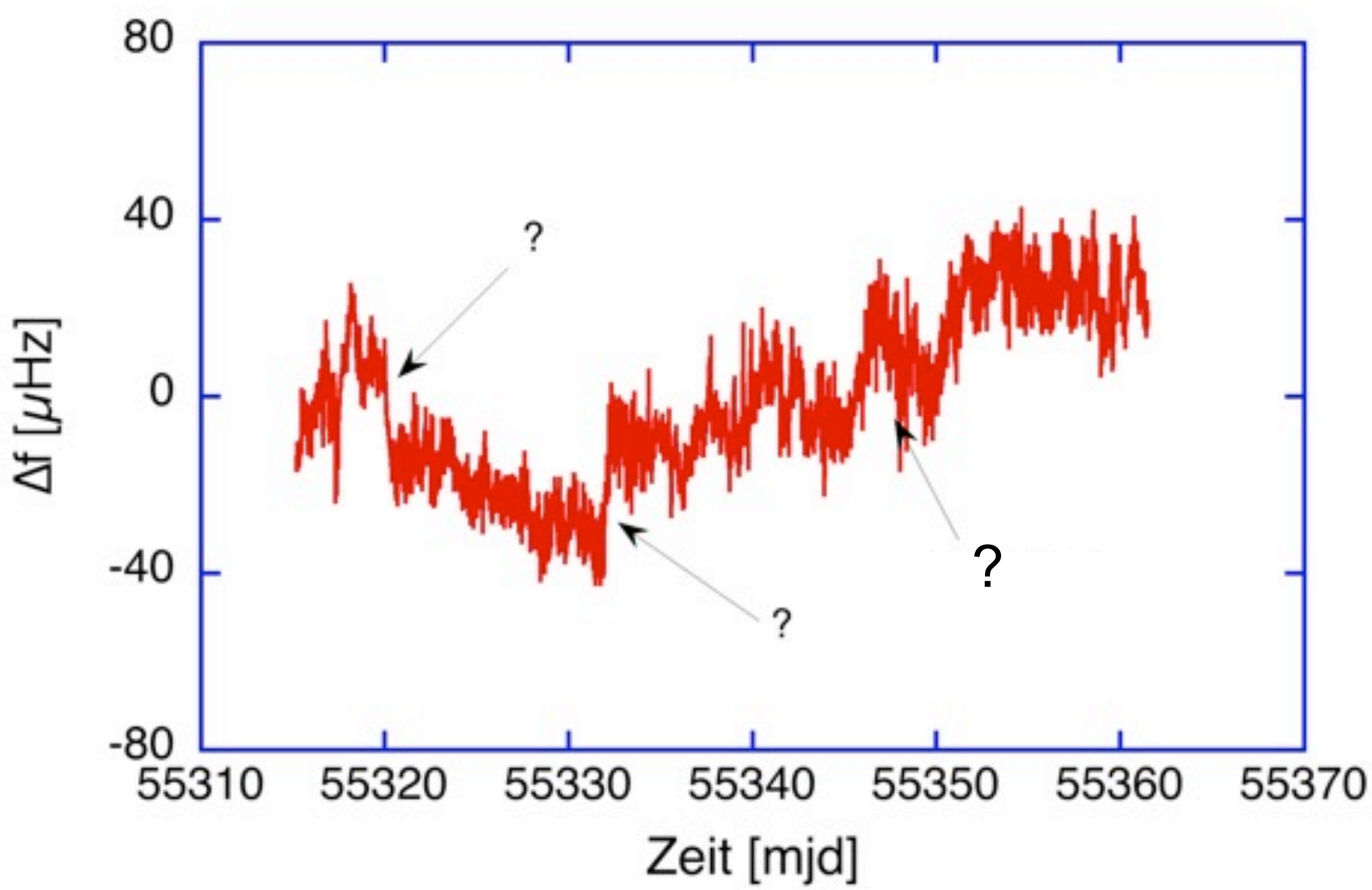

- adjustment not tight enough?
- we need a stabilization of the 4 sides rather than the integral perimeter!

Application of Optical Frequency Comb Technology

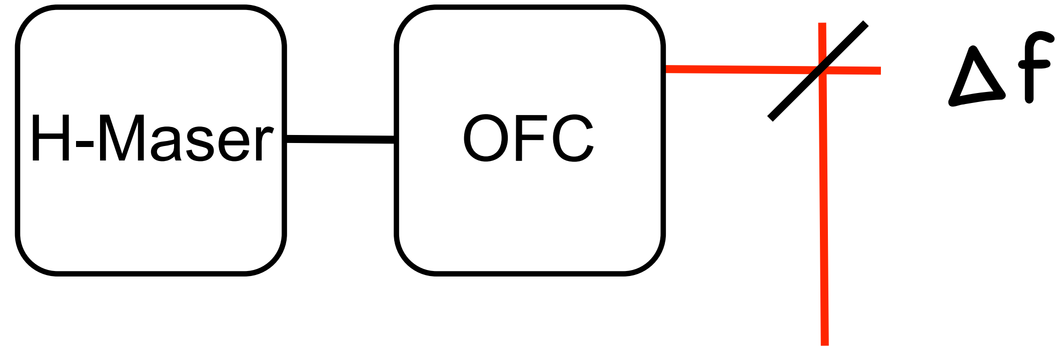

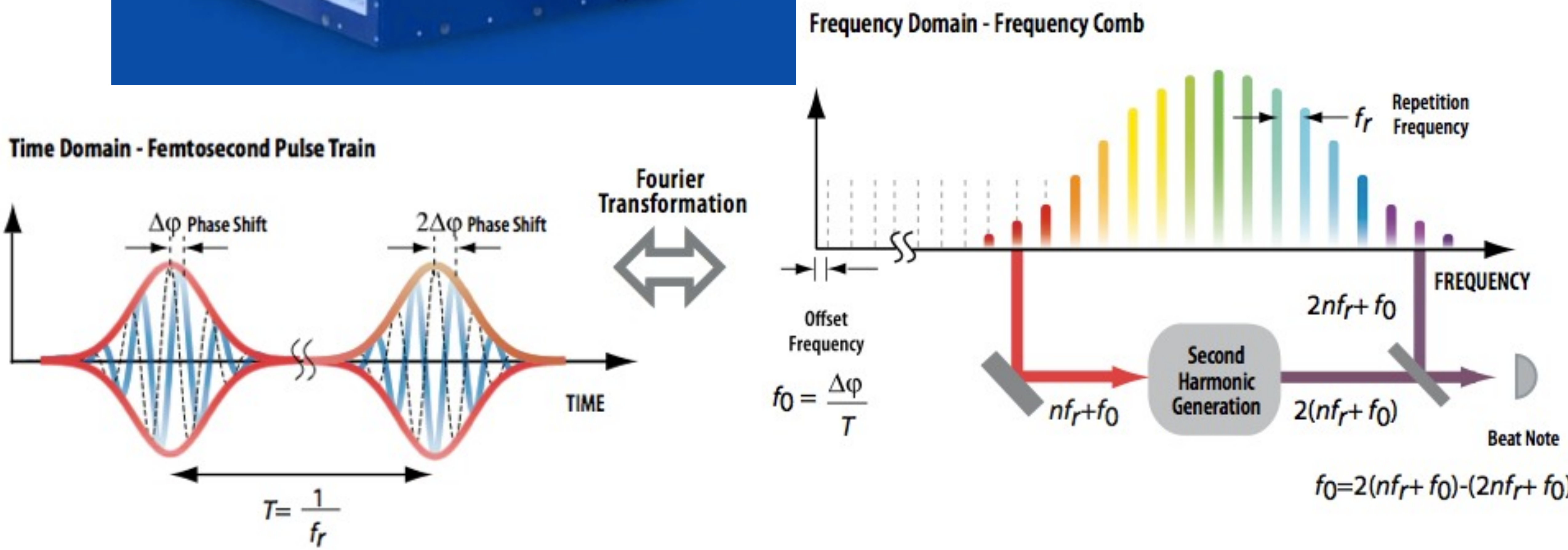

Free running RLG under open atmosphere

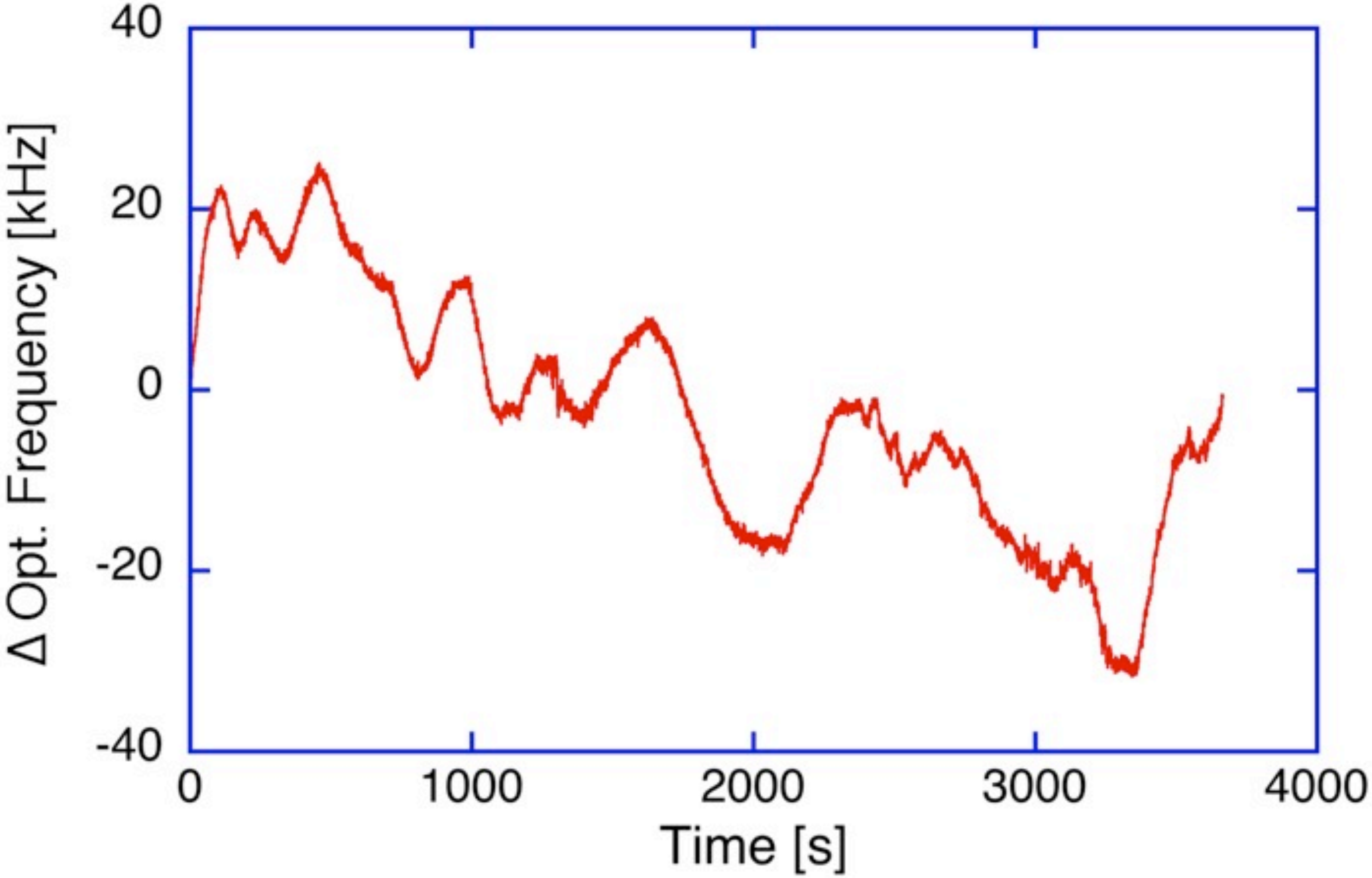

current stabilization scheme

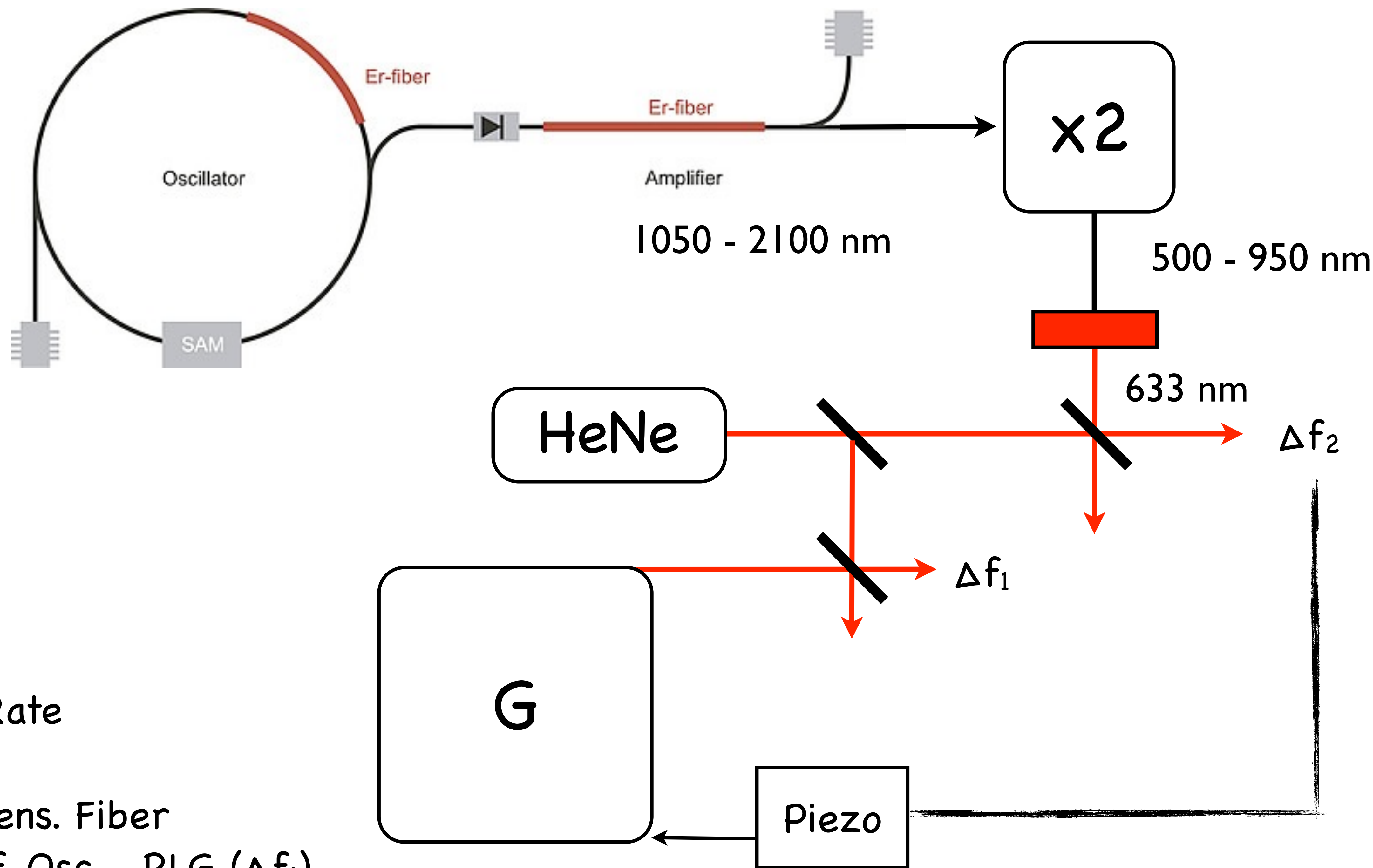

Loop 1: Rep. Rate
Loop 2: CEO
Loop 3: Compens. Fiber
Loop 4: Transf. Osc – RLG (Δf_1)
Loop 5: Transf. Osc – Comb (Δf_2)

Ring laser locked to the OFC

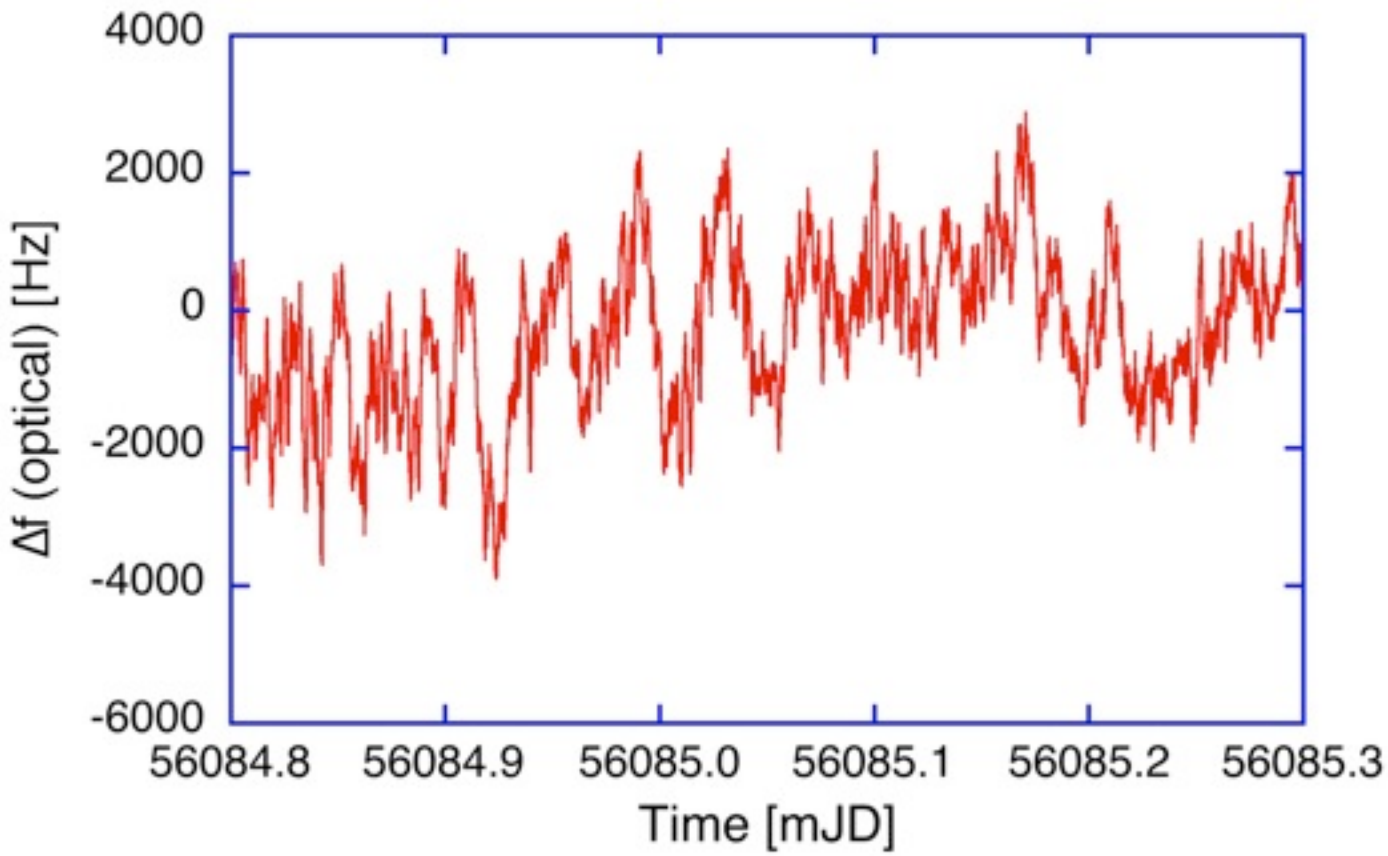

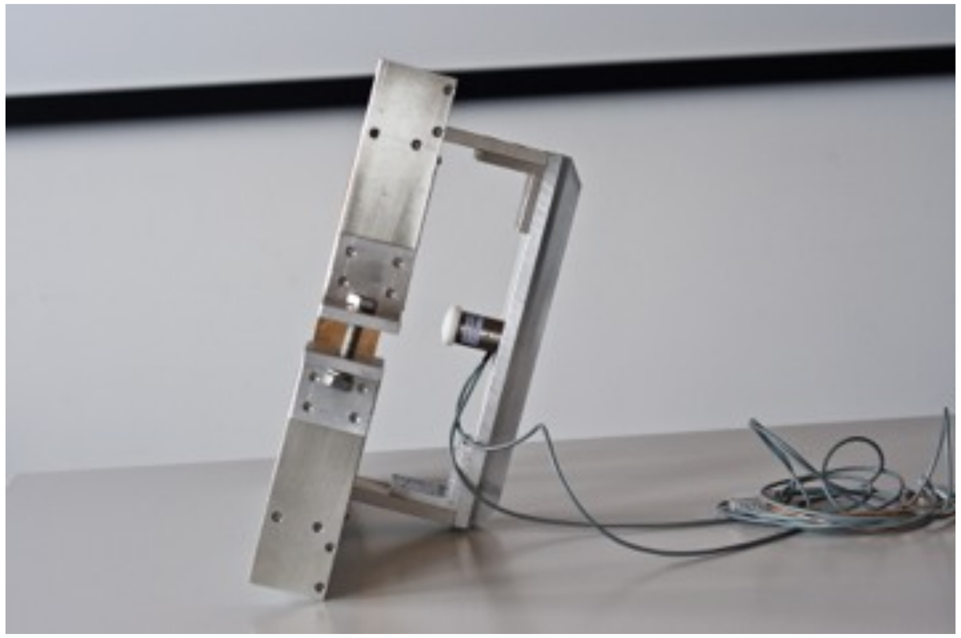

Raw data in 2012

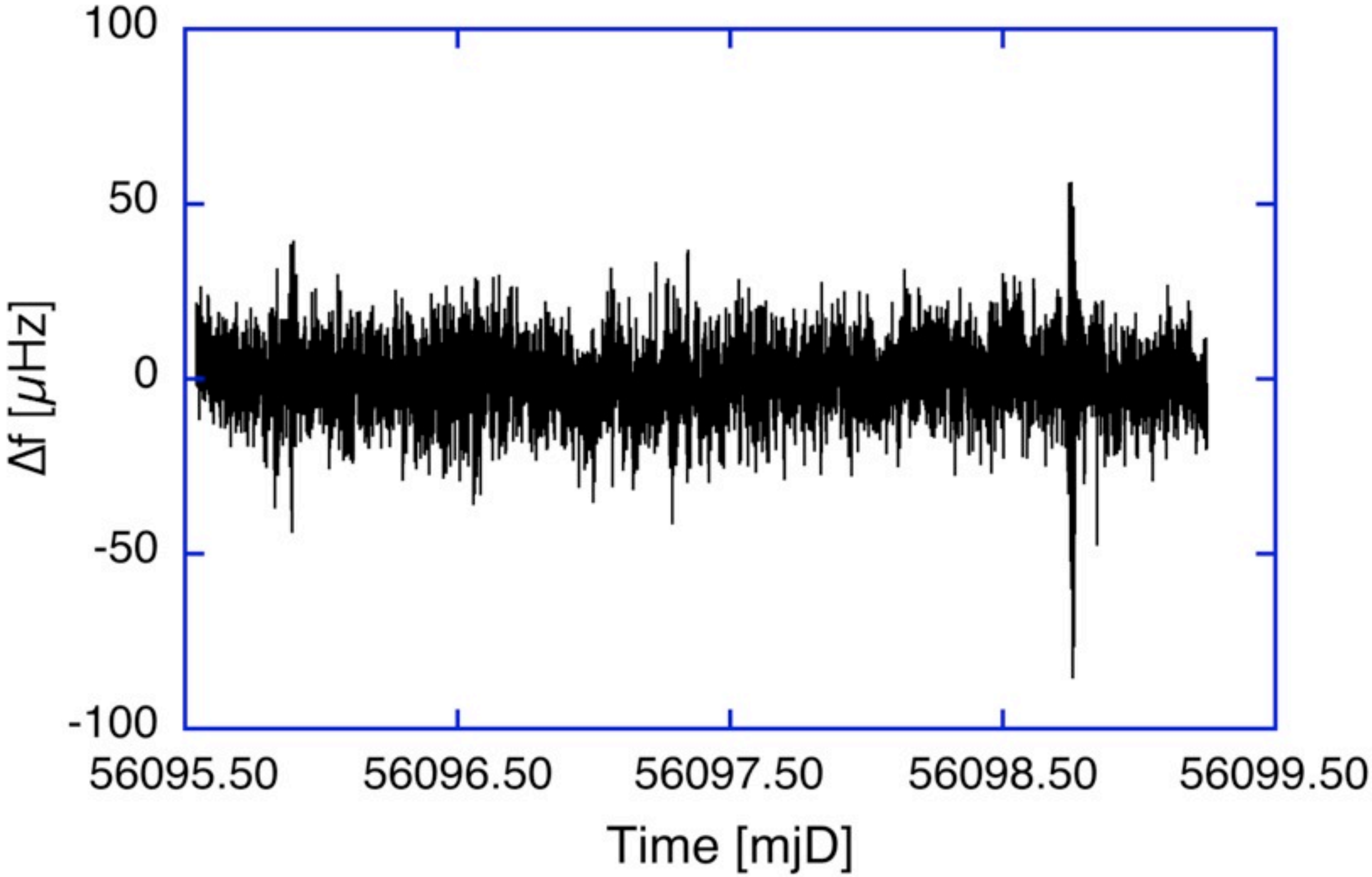

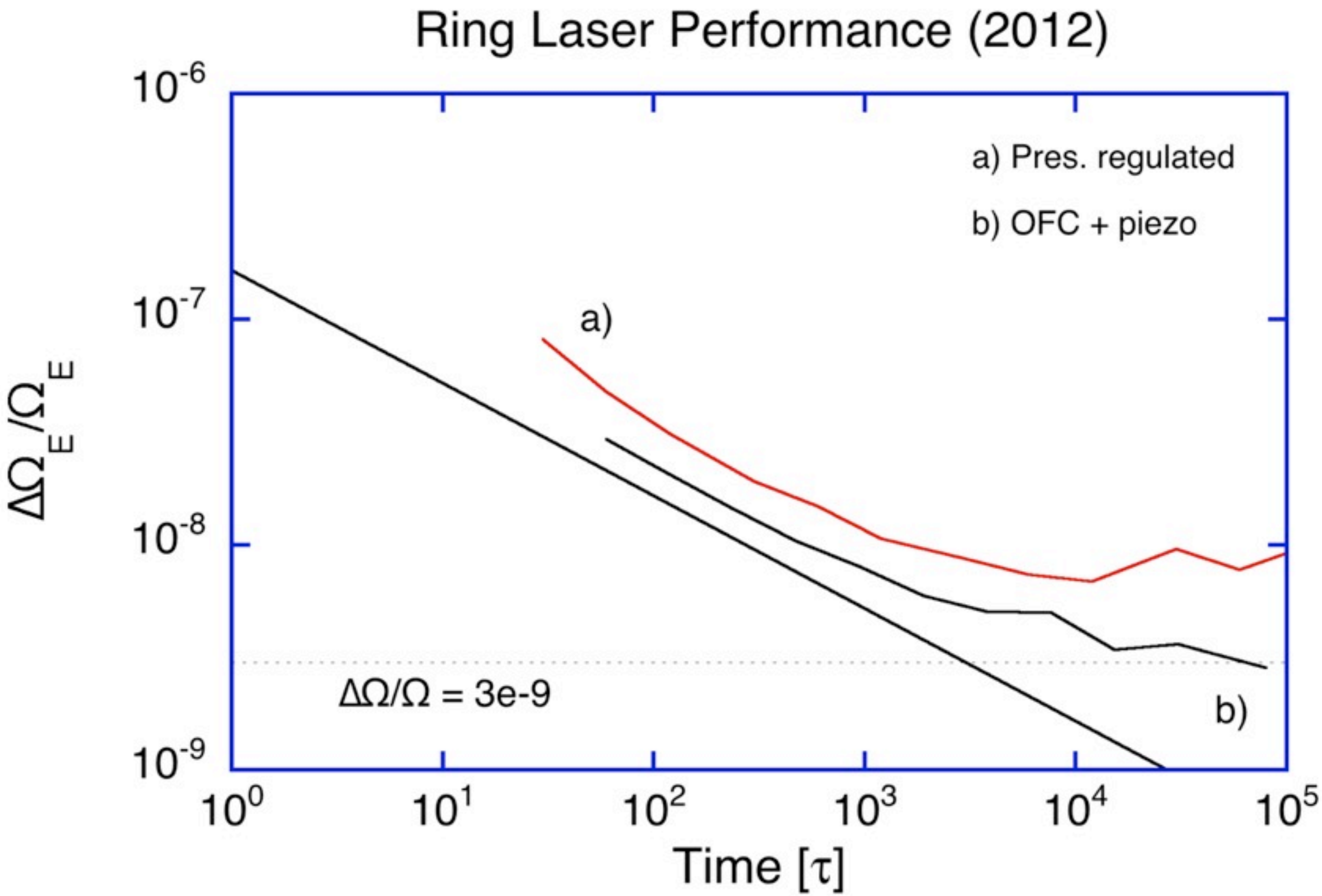

Ring Laser Performance (2012)
a) Pres. regulated
b) OFC + piezo
a)
b)
ΔΩ/Ω = 3e-9
$\Delta\Omega_E/\Omega_E$
Time [τ]
10^{-6}
10^{-7}
10^{-8}
10^{-9}
10^{0}
10^{1}
10^{2}
10^{3}
10^{4}
10^{5}